

AD-A018 281

EVALUATION OF HIGH-RESOLUTION EARTH RESISTIVITY  
MEASUREMENT TECHNIQUES FOR DETECTING SUBSURFACE  
CAVITIES IN A GRANITE ENVIRONMENT

Lewis S. Fountain

Southwest Research Institute

Prepared for:

Army Mobility Equipment Research and  
Development Center  
Advanced Research Projects Agency

15 December 1975

DISTRIBUTED BY:

**NTIS**

National Technical Information Service  
U. S. DEPARTMENT OF COMMERCE

350093

AD

**EVALUATION OF HIGH-RESOLUTION  
EARTH RESISTIVITY MEASUREMENT TECHNIQUES  
FOR DETECTING SUBSURFACE CAVITIES  
IN A GRANITE ENVIRONMENT**

by  
**Lewis S. Fountain**

**FINAL TECHNICAL REPORT**  
**Contract No. DAAG53-75-C-0213**  
**SwRI Project 14-4250**

**Prepared for**  
**Advanced Research Projects Agency**  
**1400 Wilson Blvd.**  
**Arlington, Va. 22209**

**and**

**Countermine/Counter Intrusion Dept.**  
**Mine Detection Division**  
**U.S. Army Mobility Equipment**  
**Research and Development Center**  
**Fort Belvoir, Virginia 22060**

**15 December 1975**

**Approved for public release; distribution unlimited.**

Reproduced by  
**NATIONAL TECHNICAL  
INFORMATION SERVICE**  
US Department of Commerce  
Springfield, VA. 22151

**DDC**  
**RECEIVED**  
**DEC 12 1975**  
**RECEIVED**  
**A**

ADA018281

UNCLASSIFIED

SECURITY CLASSIFICATION OF THIS PAGE (When Data Entered)

REPORT DOCUMENTATION PAGE		READ INSTRUCTIONS BEFORE COMPLETING FORM
1. REPORT NUMBER Final Technical Report	2. GOVT ACCESSION NO.	3. RECIPIENT'S CATALOG NUMBER
4. TITLE (and Subtitle) Evaluation of High Resolution Earth Resistivity Measurement Techniques for Detecting Subsurface Cavities in a Granite Environment		5. TYPE OF REPORT & PERIOD COVERED Final Technical Report 12 May 1975-15 Dec. 1975
7. AUTHOR(s) Lewis S. Fountain		6. PERFORMING ORG. REPORT NUMBER Project 14-4250
9. PERFORMING ORGANIZATION NAME AND ADDRESS Southwest Research Institute P. O. Drawer 28510, 8500 Culebra Road San Antonio, Texas 78284		8. CONTRACT OR GRANT NUMBER(s) DAAG53-75-C-0213
11. CONTROLLING OFFICE NAME AND ADDRESS Mine Detection Division, U.S. Army Mobility Equipment Research and Development Center, Ft. Belvoir, Va. 22060		10. PROGRAM ELEMENT, PROJECT, TASK AREA & WORK UNIT NUMBERS
14. MONITORING AGENCY NAME & ADDRESS (if different from Controlling Office)		12. REPORT DATE 15 December 1975
		13. NUMBER OF PAGES 77
		15. SECURITY CLASS. (of this report) Unclassified
		15a. DECLASSIFICATION/DOWNGRADING SCHEDULE
16. DISTRIBUTION STATEMENT (of this Report)  Approved for public release; Distribution unlimited.		
17. DISTRIBUTION STATEMENT (of the abstract entered in Block 20, if different from Report)		
18. SUPPLEMENTARY NOTES		
19. KEY WORDS (Continue on reverse side if necessary and identify by block number) Earth resistivity      Borehole resistivity measurements Pole-dipole electrode array      Surface remote sensing Subsurface Cavity detection Tunnel detection in granite		
20. ABSTRACT (Continue on reverse side if necessary and identify by block number)  The purpose of this work was to experimentally explore the use of earth resistivity measurements using a pole-dipole electrode array in the detection of deep tunnels in a granite environment. Measurements both on the ground surface and in drilled holes were evaluated. Tests were conducted at two sites over existing mine adits or tunnels, one at the Colorado School of Mines Experimental Mine site and one at a Gold Hill, Colorado, site. The mine adits with an approximate 10 x 10-foot		

DD FORM 1 JAN 73 1473

EDITION OF 1 NOV 65 IS OBSOLETE

UNCLASSIFIED

SECURITY CLASSIFICATION OF THIS PAGE (When Data Entered)

(3 x 3-m) cross section were successfully detected from the surface at both locations through overburden thicknesses ranging from 30 to 81 feet (9.1 to 24.7 m). Other geological features of the terrain were also identified by the measurements. Successful detection was also made from a dry borehole that was 16 feet (4.9 m) horizontally displaced from the adit at the adit level.

Although near surface geological features produce strong resistivity anomalies, they can be identified. Small tunnels in granite can be detected and located to depths approaching 100 feet (30.5 m) using a pole-dipole surface electrode array. The method is equally applicable for use in boreholes; however, field conditions and drilling problems did not permit adequate testing of the borehole resistivity measurement technique. A feature of borehole measurements is that the more homogeneous environment below the ground surface eliminates many of the complexities in data interpretation. Since the sensors can be placed at or near the anticipated tunnel depth using a borehole, the only matter of concern is horizontal detection range from the hole which should at least approach that of surface surveys.



**SOUTHWEST RESEARCH INSTITUTE**  
Post Office Drawer 28510, 8500 Culebra Road  
San Antonio, Texas 78284

**EVALUATION OF HIGH-RESOLUTION  
EARTH RESISTIVITY MEASUREMENT TECHNIQUES  
FOR DETECTING SUBSURFACE CAVITIES  
IN A GRANITE ENVIRONMENT**

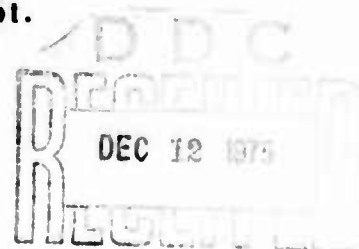
by  
**Lewis S. Fountain**

**FINAL TECHNICAL REPORT**  
**Contract No. DAAG53-75-C-0213**  
**SwRI Project 14-4250**

Prepared for  
**Advanced Research Projects Agency**  
1400 Wilson Blvd.  
Arlington, Va. 22209

and

**Countermine/Counter Intrusion Dept.**  
**Mine Detection Division**  
**U.S. Army Mobility Equipment**  
**Research and Development Center**  
**Fort Belvoir, Virginia 22060**



A

**15 December 1975**

**Approved for public release; distribution unlimited.**

## FOREWORD

The research covered by this report was performed under United States Army Mobility Equipment Research and Development Contract DAAG53-75-C-0213, funded under Advanced Research Projects Agency Order 3028. The subject is the detection of deep tunnels in granite.

The work was conducted by members of the Geoscience Systems Section of the Electronic Systems Division, Southwest Research Institute, San Antonio, Texas. Recognition is given to Institute personnel Wendell R. Peters for assistance in instrumentation development, James H. King who assisted with instrumentation, field surveying, and field measurements, Glenn T. Darilek who assisted with the field survey and layout, Francis X. Herzig who assisted with field measurements and data analysis, and Dr. Thomas E. Owen for many helpful suggestions.

Appreciation is expressed to the Colorado School of Mines for the use of the mine test site in Idaho Springs, Colorado, and to the PreMining Conditions Group of the United States Department of the Interior, Bureau of Mines for arranging for the use of a test site at Gold Hill, Colorado, and site preparation assistance.

The program was under the supervision of Dr. Ernest F. Blase of ARPA and Mr. Louis Mittelman, Jr. of USAMERDC.

## SUMMARY

The purpose of this work was to experimentally explore the use of earth resistivity measurements using a pole-dipole electrode array in the detection of deep tunnels in a granite environment. Measurements both on the ground surface and in drilled holes were evaluated.

Tests were conducted at two sites over existing mine adits or tunnels, one at the Colorado School of Mines Experimental Mine site and one at a Gold Hill, Colorado, site. The mine adits with an approximate 10 x 10-foot (3 x 3-m) cross section were successfully detected from the surface at both locations through overburden thicknesses ranging from 30 to 81 feet (9.1 to 24.7 m). Other geological features of the terrain were also identified by the measurements. Successful detection was also made from a dry borehole that was 16 feet (4.9 m) horizontally displaced from the adit at the adit level.

Although near surface geological features produce strong resistivity anomalies, they can be identified. Small tunnels in granite can be detected and located to depths approaching 100 feet (30.5 m) using a pole-dipole surface electrode array. The method is equally applicable for use in boreholes; however, field conditions and drilling problems did not permit adequate testing of the borehole resistivity measurement technique. A feature of borehole measurements is that the more homogeneous environment below the ground surface eliminates many of the complexities in data interpretation. Since the sensors can be placed at or near the anticipated tunnel depth using a borehole, the only matter of concern is horizontal detection range from the hole which should at least approach that of surface surveys.

## TABLE OF CONTENTS

	<u>Page</u>
FOREWORD	iii
SUMMARY	v
I. INTRODUCTION	1
II. EARTH RESISTIVITY SEARCH METHOD USING THE POLE-DIPOLE ELECTRODE ARRAY	3
A. General Background	3
B. Pole-Dipole Earth Resistivity Electrode Array	3
1. Theory and Method	3
2. Graphical Data Analysis	6
3. Application in Boreholes	11
a. Method	11
b. Detection Parameters	13
C. Instrumentation	14
1. DC Instrument	14
2. AC Instrument	18
III. FIELD TESTS	23
A. Idaho Springs, Colorado, Site	23
1. Site Description	23
2. Site Preparation	23
3. Resistivity Surveys and Results	29
B. Gold Hill, Colorado, Site	38
1. Site Description	38
2. Site Preparation	41
3. Resistivity Surveys and Results	41

# Table of Contents (cont. )

	<u>Page</u>
IV. CONCLUSIONS	49
V. RECOMMENDATIONS	51
A. Additional Experiments and Studies	51
B. Study the Resistivity Contrasts Between Earth Materials Associated with Cavity Detection	52
C. Develop State-of-the-Art AC Resistivity Instrumentation	52
D. Develop a Mobile, Rolling-Contact-Electrode Earth Resistivity Survey System	53
E. Continue the Investigation of Resistivity Borehole Techniques	54
F. Undertake the Long-Range Development of a State-of-the-Art Ground Penetrating Radar for Tunnel Search Applications	54
APPENDIX A -- BASIC CONCEPTS OF ELECTRICAL EARTH RESISTIVITY MEASUREMENTS	55
DD Form 1473	71



## LIST OF ILLUSTRATIONS

<u>Figure No.</u>	<u>Title</u>	<u>Page</u>
1	Pole-Dipole Earth Resistivity Electrode Array	4
2	Sample Resistivity Traverse Data Sheet With Anomalies Marked	7
3	Example Showing Graphical Method of Locating a Resistivity Anomaly	9
4	Simplified Illustration of Single-Borehole High Resolution Resistivity Measurement Method	12
5	Earth Resistivity Instrument and Accessories Set Up for Operation in the Field	16
6	Metal Current Electrodes and Porous-Pot Potential Electrodes Used with the Earth Resistivity Instrument	17
7	Photograph of a Borehole Resistivity Potential Electrode	20
8	View of the Colorado School of Mines Test Site Showing Adit Entrance	24
9	View of the Colorado School of Mines Test Site Showing the Rugged Surface and Steep Slope	25
10	View of Mine Shaft Showing Granite Outcropping	26
11	Contour Map of the Area Over the Mine at Idaho Springs, Colorado	27
12	Contour Map of the Sloping Surface from Mine Entrance to Service Road	28
13	Graphical Pole-Dipole Resistivity Survey Results for Traverse Along Service Road Crossing Mine Adit (Colorado School of Mines Experimental Mine)	30

# List of Illustrations (cont. )

<u>Figure No.</u>	<u>Title</u>	<u>Page</u>
14	Interpretation of Resistivity Data Along Traverse A, Idaho Springs, Colorado (Only resistivity high's caused by mine are shown)	32
15	Graphical Pole-Dipole Resistivity Survey Results for Traverse Along Row "B" Perpendicular to Mine Adit Center Line (Colorado School of Mines Experimental Mine)	33
16	Sectional Views of Borehole Detection Results, Idaho Springs, Colorado	34
17	Photograph of Gold Hill Test Site Looking Southeast Along Survey Line 3	39
18	View Showing a Large Crater Near Resistivity Traverse Lines at the Gold Hill, Colorado Test Site	40
19	Topographical Map of the Gold Hill, Colorado Test Area	42
20	Sketch of Earth Resistivity Interpretation of a Traverse Along Survey Line 7, Gold Hill, Colorado	43
21	Resistivity Data Graphs of the Southwest End of Line 7 Traverse, Gold Hill, Colorado	45
22	Resistivity Data Graphs of the North East End of Line 7 Traverse, Gold Hill, Colorado	46
A-1	The Wenner Electrode Array	61
A-2	The L-Shaped Electrode Array	64
A-3	The Switched-Electrode Equatorial Dipole Array	67

## I. INTRODUCTION

Detecting and mapping of underground irregularities from the earth's surface are of special interest to military groups involved in locating man-made tunnels used in guerrilla warfare. The problem is also of interest to highway construction engineers, archeologists, speleologists, and mining and petroleum exploration crews. As important as this problem is, no completely satisfactory solution has been found. A part of the problem lies in the complex structure of the earth's thin aerated top soil which varies greatly in physical structure from area to area and even within a given area making exploration data difficult to interpret. Geophysicists, whose general interests entail much greater penetration depths, usually ignore the first 5- to 50-foot (1.5- to 15.2-m) layer of soil by assigning a correction factor to their data to account for errors involved. Consequently, little detailed information has been published in the literature concerning the small scale characteristics of the earth's top layer of soil.

One characteristic used to classify the earth's substructure is its apparent electrical resistivity as measured from the surface. Measurements of earth resistivity have been used for many years to map subsurface stratigraphic irregularities. They can provide a quantitative measure of the conducting properties of the subsurface and can be used to map the depth to horizons having anomalously high or low conductivity. The method has been used to locate and map faults, shallow oil structures, gravel beds, stratification, mineralized faults, water table depth, and to locate the depths of transition from fresh to salt water in fluid saturated formations. Although the measurement method is simple, it has not been used extensively to explore the first few feet below the earth's surface.

Southwest Research Institute completed a series of field tests in June 1975 to evaluate a high-resolution pole-dipole earth resistivity survey technique for detecting and mapping sinkhole cavities in connection with highway routing and maintenance problems<sup>1</sup>. Analysis of the test results obtained with this surface-operated geophysical

---

<sup>1</sup> L. S. Fountain, F. X. Herzig, and T. E. Owen, "Detection of Subsurface Cavities by Surface Remote Sensing Techniques," Report No. FHWA-RD-75-80, SwRI Final Technical Report, Contract No. DOT-FH-11-8496, Southwest Research Institute Project 14-4250, June 1975.

measurement method showed excellent success in locating small underground solution cavities in Florida limestone and in locating subsurface cavities and other geologic anomalies along highway rights-or-way in Alabama and Florida. A graphical analysis was used that allowed the position of the detected voids to be determined.

This same method had been successfully used to locate solution cavities in limestone environments by Bates<sup>2</sup> and Bristow<sup>3</sup>.

A problem of concern to the United States Army is the detection of cavities and tunnels in granite at depths of from a few feet (about 1 metre) to greater than 150 feet (45.7 m) below the ground surface. Cross sections of these targets are in the range 6 x 6 feet (1.8 x 1.8 m) to 10 x 10 feet (3 x 3 m). These depths and target dimensions were in the range of detection capabilities of the earth resistivity method, but such measurements had not been evaluated in a granite environment.

It was the purpose of this program to evaluate earth resistivity search techniques as a possible solution to the detection of deep tunnels in granite.

The scope of the program covered the buildup of simple instrumentation for field data collection; collection of earth resistivity data both in boreholes and on the earth's surface at two test sites in Colorado; and simple graphical analysis of the collected data.

---

<sup>2</sup> E. R. Bates, "Detection of Subsurface Cavities," Miscellaneous Paper S-73-40, AD 762538, U. S. Army Engineer Waterways Experiment Station, Vicksburg, Mississippi, June 1973.

<sup>3</sup> C. Bristow, "A New Graphical Resistivity Technique for Detecting Air-Filled Cavities," *Studies in Speleology*, 1, Part 4, 204-227, December 1966.

## II. EARTH RESISTIVITY SEARCH METHOD USING THE POLE-DIPOLE ELECTRODE ARRAY

### A. General Background

A variety of electrical resistivity geophysical exploration methods have been explored as possible approaches to subsurface cavity detection. The basic resistivity measurement and analysis concept underlying these various attempts has been essentially the same in each case: that is, by establishing an otherwise predictable electrical current distribution within a relatively large volume of homogeneous earth material, any observed perturbations in the current distributions measured as potentials or electric fields at the ground surface can be interpreted in terms of possible subsurface structural or earth material resistivity anomalies. The degree of perturbation in the current distribution is dependent upon the resistivity contrast between the anomalous subsurface structures and the surrounding earth material; and, equally important, the detectability of such perturbations is also dependent upon the size and shape of the anomaly and its orientation relative to the current flow.

The main differences among the various electrical resistivity geophysical profiling methods are largely in the electrode array patterns used to establish the subsurface current distributions and in measuring the potential differences at the ground surface. The manner in which the electrodes are moved or scanned over the area being surveyed also differs with the different electrode arrays as do the methods of resistivity data analysis and interpretation.

Detailed descriptions and discussions of various electrical resistivity methods of subsurface cavity detection are presented in Appendix A.

The pole-dipole array has had less previous use and has shown the greatest potential for detecting underground cavities and predicting their depths and locations. This method will be discussed in detail below.

### B. Pole-Dipole Earth Resistivity Electrode Array

#### 1. Theory and Method

The pole-dipole electrical resistivity survey



method is based on a four-electrode array configuration in which the current sink electrode is located at effective infinity, and the potential electrodes are separated from one another by a fixed minimum distance proportional to the desired resolving power of the system. The potential electrode pair is located at various positions along a selected line near the current source electrode as the means of vertically sounding the subsurface below that electrode. The current source electrode is then moved ahead along the line at suitable incremental distances to provide horizontal profile scanning. The pole-dipole array is illustrated in Figure 1. In order that the

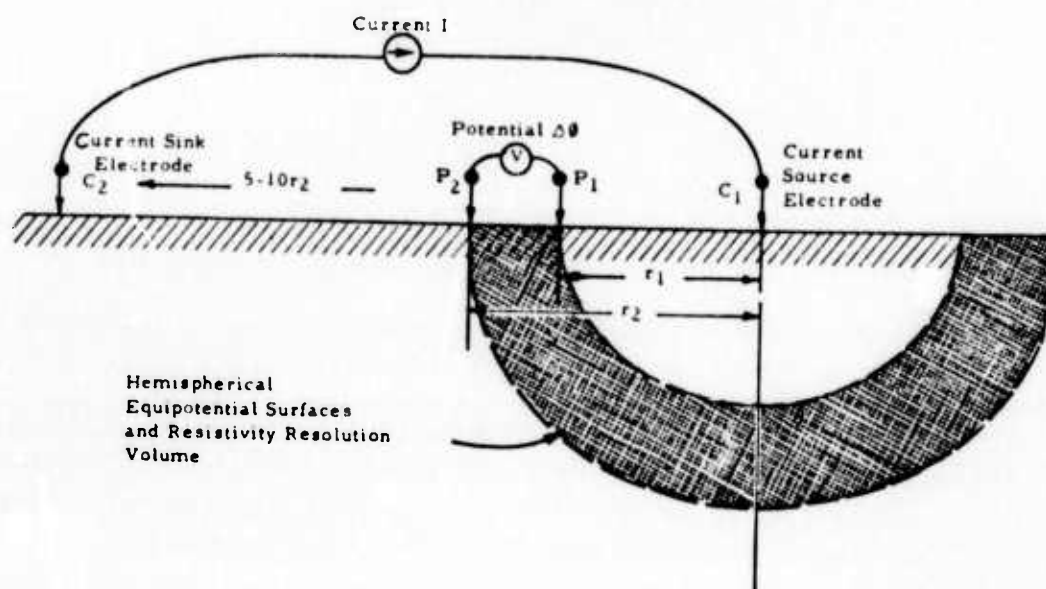


FIGURE 1. POLE-DIPOLE EARTH RESISTIVITY ELECTRODE ARRAY

equipotential surfaces be hemispherical and concentric about the source electrode, the sink electrode must be located at effective infinity which will generally be about 5 to 10 times the largest value of detection penetration depth of interest in the survey. In a typical survey, the potential electrode pair is spaced at a fixed separation of 20 feet (6.1 m) and moved away from the source electrode at 10-foot (3-m) intervals to provide overlapping and redundant resistivity data.

A modified form of this array has been used to improve the reliability and accuracy of detecting small subsurface cavities. The modifications pertain largely to the collection of overlapping field data using closer potential electrode spacings. These overlapping measurements are elaborate enough to provide up to four different potential electrode pair readings at each measurement station for refinement of the resistivity interpretation analysis. This modification also entails measurements on both sides of the source electrode. This is the method used by SwRI in the work reported in Reference 1 and in the work covered by this report. For clarity of explanation, the overlapping survey procedure is described as follows for a typical 100-foot (30.5-m) penetration depth survey:

- a. Place the current source electrode,  $C_1$ , as shown in Figure 1, at the first traverse station;
- b. Place the current sink electrode,  $C_2$ , at a minimum distance of 500 feet (152.4 m), (5  $r_2$ ), behind  $C_1$  on the pre-established traverse line having already decided that the maximum potential electrode scan distance from  $C_1$  will be 100 feet (30.5 m);
- c. Place potential electrodes,  $P_1$  and  $P_2$ , at pre-established station markers at 10 feet (3 m) and 20 feet (6.1 m), respectively, on the sink electrode side of  $C_1$ , and obtain resistance reading;
- d. Repeat step c above with potential electrodes,  $P_1$  and  $P_2$ , at pre-established station markers at 20 feet (6.1 m) and 30 feet (9.1 m), respectively, on the sink electrode side of  $C_1$ , and obtain resistance reading. Continue movement of the  $P_1$  and  $P_2$  electrodes in this manner until the final potential reading is obtained at 90 feet (27.4 m) and 100 feet (30.5 m) from  $C_1$ ;
- e. Next, place potential electrodes at pre-established 10-foot (3-m) interval station markers on the opposite side of  $C_1$  from  $C_2$ , and obtain resistance readings at each station pair out to the 100-foot (30.5-m) limit. This completes the survey procedure for the first current station position for  $C_1$ ;
- f. Move  $C_1$  up the traverse line a distance of 40 feet (12.2 m), and obtain resistance readings over the 100-foot (30.5-m) scan zones on each side of this current station;

g. Repeat step f above until complete traverse line is surveyed.

The above survey procedure gives four overlapping resistance readings for each 10-foot (3-m) spaced potential electrode pair station to a depth of more than 50 feet (15.2 m) as the survey proceeds. This procedure with both 5- and 10-foot (1.5- and 3-m) potential electrode spacing was used in all of the pole-dipole earth resistivity tests performed on this program. The bi-directional potential scanning doubles the amount of data per current station over that obtained by earlier procedures. The four-level data overlap aids in resolving the locations and resistivity contrasts of the various high- and low-resistivity anomalies which may be encountered along the traverse. This is accomplished by the multiple positional aspect observations of possible anomalies as detected from several survey stations; whereas, in contrast, for less redundant observations a high-resistivity anomaly and a low-resistivity anomaly occurring in the same hemispherical shell field of view will tend to nullify one another and be undetected.

A straightforward graphical analysis method was devised capable of utilizing and displaying all of the field data as a means for locating the experimental best-fit positions and depths of detected subsurface cavities. The success of this analysis approach is largely achieved through the spatial redundancy of the field data with the result that target ambiguities and false interpretations are minimized, and improved cavity size and shape indications are derived.

## 2. Graphical Data Analysis

The graphical analysis of the pole-dipole resistivity data can best be illustrated by first examining a sample of field data. The basic field measurements as performed on this program were recorded on specially prepared data forms. Figure 2 is a sample data sheet showing recorded instrument readings, calculated resistivity values, and a graph of a derived resistivity profile. The first column on the data sheet is the potential-pair electrode distance from the current source electrode; the second column lists the distances from current electrode to midpoint between potential electrodes; the third column is the resistivity instrument reading in ohms (or in volts if AC instrumentation is used); the fourth column is the geometrical factor required to calculate apparent resistivity for the distances listed in the first column using the resistances recorded in the third column or calculated from the recorded voltage and earth current for AC instrumentation; and the fifth column is the calculated value of apparent resistivity in ohm-centimeters  $\times 10^3$  ( $\Omega \cdot m \times 10$ ).

PROJECT 14-4250  
 TEST NO. 2  
 DATE 17 June 1975  
 WEATHER CONDITIONS Cloudy-Cool, About 50°

SITE Colorado School of Mings  
 AREA Service Road Crossing Adit  
 CURRENT PROBE POSITIONS 000-600; 000 + 10  
 GOSERVER F & H

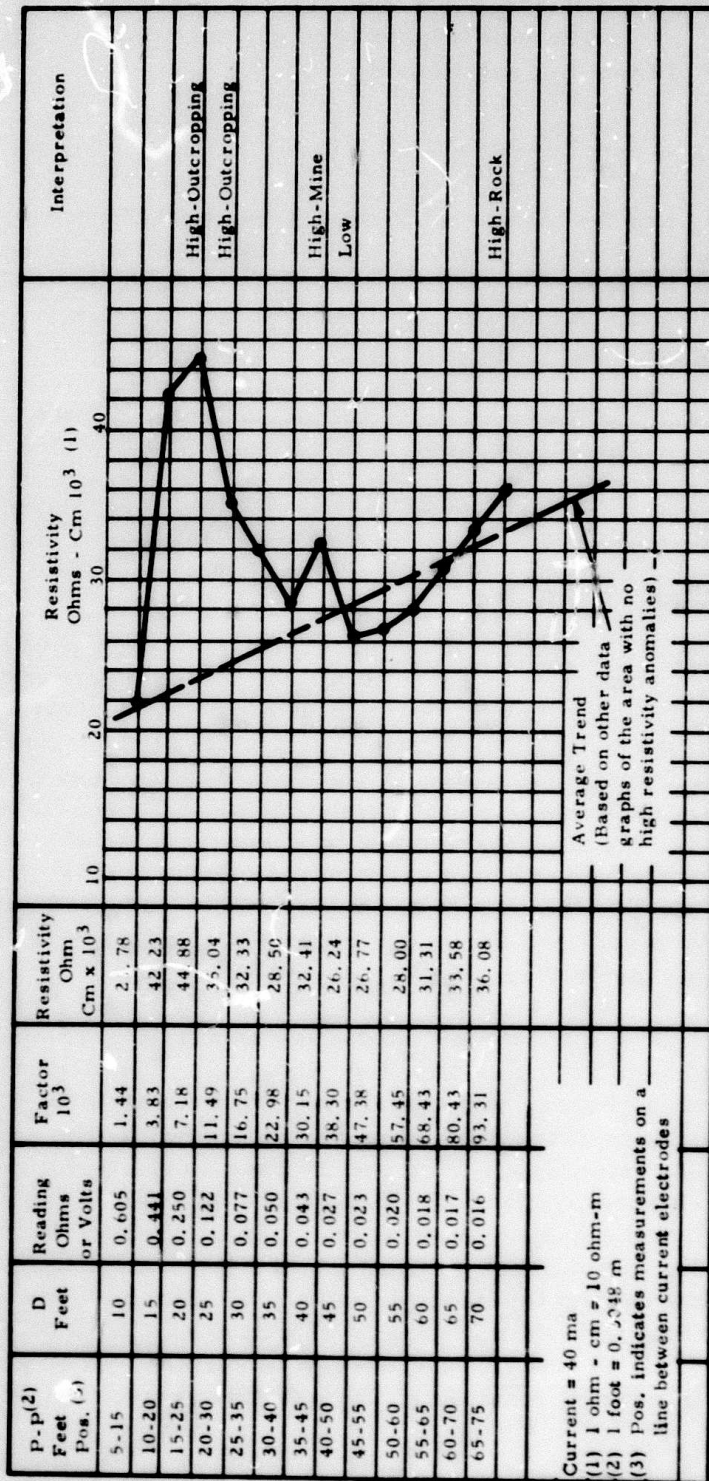


FIGURE 2. SAMPLE RESISTIVITY TRAVERSE DATA SHEET  
 WITH ANOMALIES MARKED



The pole-dipole geometrical factor in column four is calculated from the relationship,

$$K = \frac{2\pi r_1 r_2}{r_2 - r_1} \quad (1)$$

where  $r_1$  and  $r_2$  are the distances of the potential electrodes,  $P_1$  and  $P_2$ , from the current source electrode,  $C_1$ , as illustrated in Figure 1. The basic principles on which the geometrical factor,  $P$ , is derived are discussed in Appendix A and applied to several earth resistivity electrode array configurations.

Apparent resistivity is calculated from the equation developed in Appendix A

$$\rho = KR \quad (2)$$

where  $R$  is the measured resistance.

A graph of the apparent resistivity profile on one side of the current source electrode is plotted on the data sheet as shown in Figure 2. Those points on the profile that indicate high or low resistivity perturbations away from the average profile trend are next identified and marked for transfer to a scaled drawing used to graphically locate the anomalous underground resistivity structures. Determinations of the average profile trends are made by visual inspection. A simple and liberal interpretation of high and low resistivity perturbations is permissible since the redundancy of the data and a required multiplicity of perturbations associated with each underground anomaly will delete the improper interpretations.

An example of the scaled drawings used in the graphical analysis is set up as shown in Figure 3. The distance along the ground surface representing the survey traverse is marked, and the consecutive positions of the current probe are shown by the arrows. The perturbations interpreted from the forward and reverse resistivity profiles for each current electrode station are denoted on the bracketed lines drawn above the ground surface line. The high resistivity anomalies in this example are labeled as A, B, C, and D as taken from the related data graphs shown at the top of the illustration. The data in this example are actual field data that show detection of a 10 x 10-foot (3 x 3-m) mine adit 30 feet (9.1 m) below the surface. With a compass centered at each current location on the ground surface line, arcs are



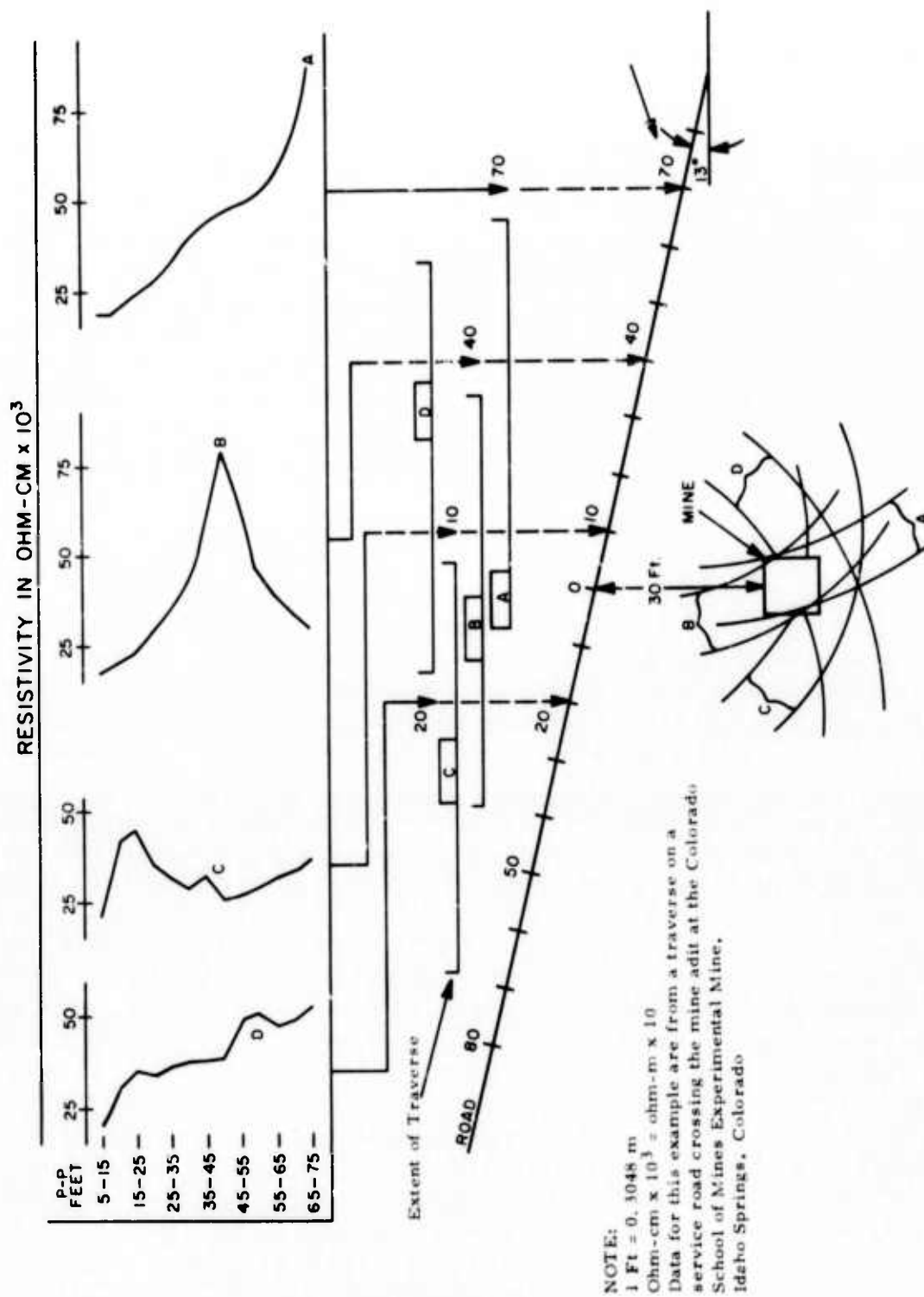


FIGURE 3. EXAMPLE SHOWING GRAPHICAL METHOD OF LOCATING A RESISTIVITY ANOMALY

drawn at distances representing the bounds of the high resistivity anomaly with respect to the current probe position. The pairs of circular arcs are labeled A, B, C, and D corresponding to the interpreted anomalies. The space where the four sets of arcs intersect is the graphically derived location of the underground structure responsible for the high resistivity perturbations. Indeed, a useful arbitrary guide for taking advantage of the redundancy of the overlapping field measurements is to require a minimum of three arcs to intersect at a common anomaly location before it is interpreted with any confidence as a probable underground cavity. Moreover, as illustrated in Figure 3 the arcs are drawn only in the 90-degree sectors corresponding to either the forward or reverse profiles containing the perturbations being used. The reason for this is that the distortions of the equipotential lines (represented in a first order manner by the circular arcs) are very weak if the perturbing anomaly is located in the opposite 90-degree sector.

It should be recognized that the pairs of arcs drawn for each resistivity perturbation not only describe the resistivity perturbations in the vertical plane along the ground traverse line but applies, to some extent, to a three-dimensional spherical shell segment extending laterally on each side of the traverse line. It has been speculated by both Bristow and Bates that this apparent lateral field of view away from the traverse line is contained within an angle of about  $\pm 25$  degrees on each side of the traverse line relative to the source current electrode location.

Detailed interpretation of the subsurface arc intersections is complex, and a knowledge of the geology of the area is almost a necessity. In many cases the high resistivity anomalies are caused by bedrock-soil interfaces, especially in locations where the bedrock elevations are very irregular. A low resistivity indication is usually a soil- or solution-(soil with a very high water content) filled cavity surrounded by otherwise higher resistivity structures such as dolomite or granite. A few test borings in the test area can be a great help in interpreting the detailed implications of the anomalies.

Errors in data interpretation can be caused by underground wires, metal fences with metal posts on the surface, buried pipes, abrupt cliffs, ponds, streams, etc. in the area surveyed. The effects of these various disturbing features is to distort the earth current patterns from the assumed spherically divergent paths postulated for a flat homogeneous ground. Interference features of this type should be avoided where possible or approached with the electrode array oriented at right angles with respect to the obstacle.

### 3. Application in Boreholes

#### a. Method

In applying the method in a single vertical borehole, a resistivity measurement cable string consisting of a current source electrode and two potential electrodes is located in the borehole; the current sink electrode is located at effective infinity on the surface as was done in the surface survey measurements. Measurements are then made by moving the fixed-space pair of potential electrodes in chosen increments away from the current source electrode. Several sets of measurements can be made in a single borehole. The current source electrode can first be placed in the bottom of the hole and resistivity measurements made upward from the bottom of the hole toward the top. The current source electrode is then placed at another location up the hole and resistivity measurements made around this new current source location. This technique is repeated up the hole until the measurements are well above the anticipated depth of the target anomaly. The sets of data can then be used with the same graphical method as is used with surface surveys to obtain a depth below surface bearing on a resistivity anomaly such as might be caused by a subsurface void.

When the method is applied below the ground surface in a homogeneous earth, the current injected at the source electrode will diverge with radial symmetry into the earth medium giving rise to concentric spherical equipotential surfaces equivalent to the hemispherical surfaces described earlier. Resistivity anomalies occurring within any two closely spaced spherical equipotential surfaces (a potential difference shell) will be observed although the azimuthal orientation of such anomalies will not be discernable until supplemental measurements are made in other nearby boreholes. From a single borehole, however, anomalous geological features can be detected, resolved in size, and located accurately in depth through the process of making overlapping and redundant resistivity measurements along the borehole. This concept is illustrated in Figure 4 where the anomalous geologic target occupies only a localized volume. Localization of the anomaly in depth is evident from the intersection of the two spherical potential shells shown; however, the intersection zone of these shells is toroidal in shape and oriented symmetrically about the borehole axis. Thus, if the azimuthal position of the target relative to the borehole axis is to be determined without ambiguity, it must be done by the intersection of at least three other similar toroidal detection zones responding to the same target as derived from resistivity measurements made in separate adjacent boreholes.

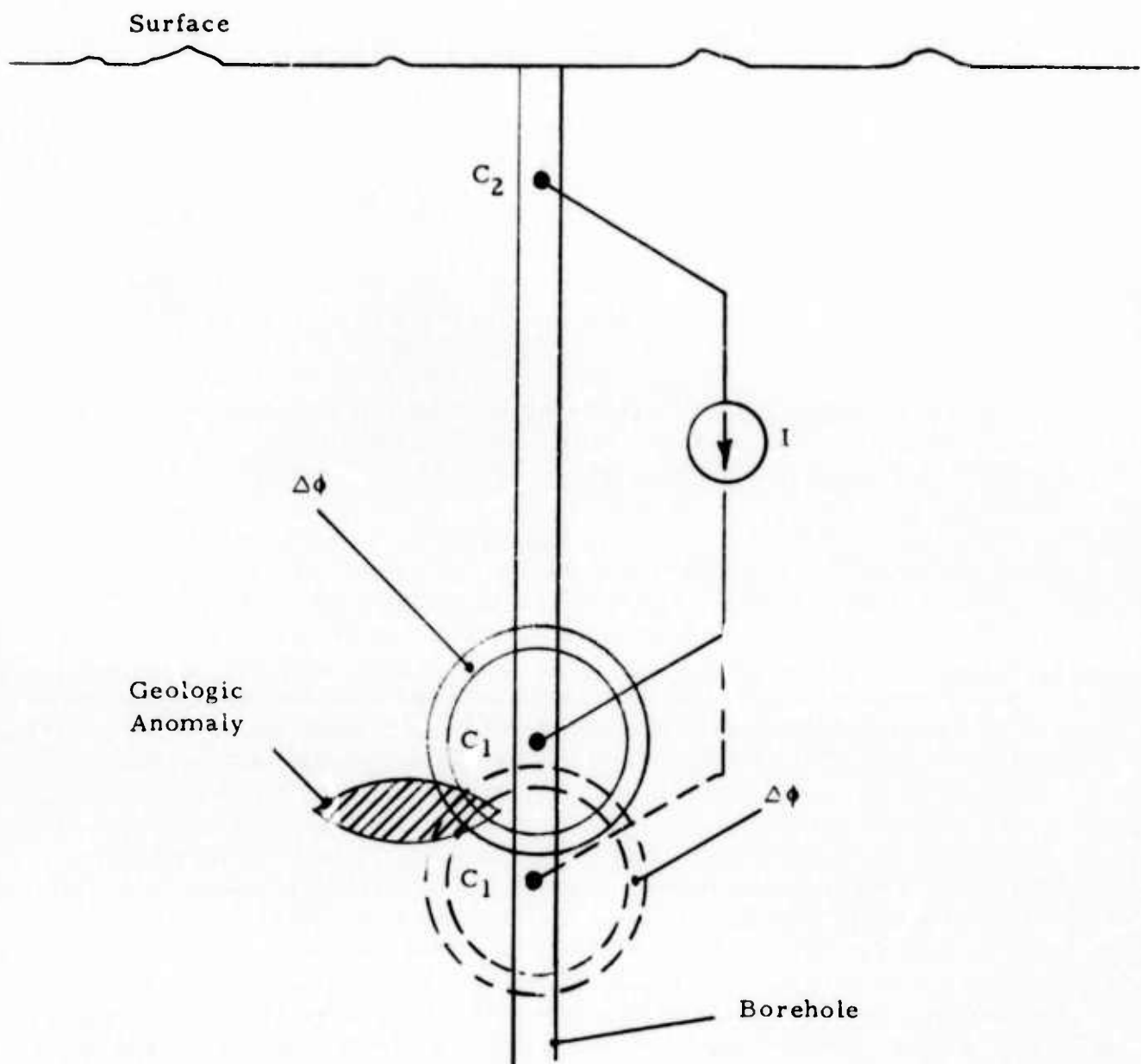


FIGURE 4. SIMPLIFIED ILLUSTRATION OF SINGLE-BOREHOLE  
HIGH RESOLUTION RESISTIVITY MEASUREMENT METHOD

The geometrical factor used in the calculation of apparent resistivity from measurements made in a borehole changes when the current source is below the surface to

$$K_B = \frac{4\pi r_1 r_2}{r_2 - r_1} \quad (3)$$

This change is because the potential difference shells around the current source electrode are now spherical in shape.

b. Detection Parameters

Many factors affect the underground detection effectiveness of any earth resistivity search method. Some of the more important factors are:

- |  |     |                               |
|--|-----|-------------------------------|
|  | (1) | Target shape                  |
|  | (2) | Target size                   |
|  | (3) | Target distance from traverse |
| line (distance from borehole or, for surface survey, depth below |     |                               |
| surface)   |     |                               |
|  | (4) | Target distance from current  |
| source   |     |                               |
|  | (5) | Potential probe spacing       |
|  | (6) | Resistivity contrast between  |
| target and background  |     |                               |

A study done by SwRI for the U. S. Bureau of Mines on another program has evaluated some of these parameters, as they relate to resistivity measurements from a borehole. A general summary of the results will be given here to provide some insight into detection possibilities.

Target shape is a critical factor as is its size. The distance to which a spherically shaped target may be detected is directly proportional to its diameter and inversely proportional to the cube root of the certainty with which the background signal can be predicted. If the geological background is sufficiently uniform that the background resistivity signal can be predicted to within 1%, then signal perturbations of 2% should be recognizable. Under such conditions a spherically-shaped target of good resistivity contrast could be detected at a distance of almost 3 radii from the borehole to the centroid of the target (or about one target diameter



distance from borehole to nearest surface of the target). A cylindrically shaped target having the same strength perturbation signal as the sphere would be detectable at a greater distance than the sphere. For example, if a 10-foot (3-m) diameter spherical void centered 15 feet (4.5 m) from the borehole produces a given signal above noise, then a long cylindrical cavity with the same diameter would produce the same signal at approximately 53 feet (16.2 m). This relationship is expressed as

$$\text{Distance to Cylinder} = K \left( \frac{\text{Distance to Sphere}}{\text{Sphere Radius}} \right)^{1/2} \text{Distance to Sphere} \quad (4)$$

where K is a function of the ratio of target and background conductivity. In the case of an air-filled void,  $K = 2$ .

Potential electrode spacing used in borehole resistivity measurements plays an important part in resolving targets. Numerical modeling has shown that for electrode spacing less than half the target sphere radius, the detection capability is essentially independent of electrode spacing. For larger spacing the sensitivity falls off linearly as probe spacing increases. As an example, the perturbation component of a processed signal for an electrode spacing equal to two target sphere radii is about one half its largest value.

It is intuitive that an air-filled void within a homogeneous volume of conducting earth material would impose a greater resistance to electric currents flowing in the vicinity of the void than in other parts of the material volume. Conversely, a water- or mud-filled void will offer a lower resistance to electric current since the conductivity of the filling material will generally be greater than that of the surrounding material. The degree of perturbation in the current distribution is, therefore, obviously dependent upon the resistivity contrast between the anomalous subsurface structures and the surrounding earth materials. The analysis showed that the ability to detect any target from a borehole is directly related to the conductivity contrast between the target and the surrounding materials.

### C. Instrumentation

#### 1. DC Instrument

Earth resistivity measurements were made using both AC and DC type instruments.

The DC measurements were made using a Keck Model 1C-69 instrument as shown set up in the field along with accessories in Figure 5. Figure 6 is a photograph showing two metal current electrodes and two porous-pot potential electrodes used with the instrument.

The commercial instrument is a DC system obtaining power for earth current from dry cell batteries. Four 45V batteries are housed in the instrument case, and there is a receptacle on the case where additional batteries can be added as required. The battery case shown on the ground to the right of the instrument in Figure 5 contains 10 additional NEDA 205, 45V batteries. Switches on the instrument panel and on the battery pack allow individual batteries to be switched into the circuit in series as required. Resistance can be measured with the instrument over the range 0.001-1000 ohms, and the dial can be read to one part per thousand.

The Keck resistivity instrument can also be used to measure self potential that often results from the electrochemical action between soil solutions and ore bodies. In nearly all cases when two electrodes are placed on the ground surface a DC potential can be observed between them. If porous-pot electrodes are used, this potential will be related to natural earth currents. The instrument contains a circuit capable of nulling out this natural earth potential so that it does not affect the resistivity measurements. The instrument dial used to adjust the indicator circuit for a null is calibrated to read in millivolts and can be read when a null is obtained. This self potential data can be of value in aiding interpretation of earth resistivity measurements collected over solution-filled cavities. The instrument has a "forward-reverse" switch on the panel to change the direction of the current flow into the earth. For precise resistance determinations, field measurements were made using both directions of current flow, and the two measurements averaged.

Another reversing switch was added as a modification to the instrument. This was done to allow faster setup of electrodes in special electrode arrays. The potential electrodes must be connected to the instrument in the proper polarity since the unit is a DC instrument, and DC nulling potentials are used. Once in operation if the two potential electrodes are reversed, as might occur if alternate electrodes are moved ahead along the survey traverse, the additional reversing switch allows the potential electrodes to be reversed independently of the current electrodes.



FIGURE 5. EARTH RESISTIVITY INSTRUMENT  
AND ACCESSORIES SET UP FOR OPERATION IN THE FIELD



FIGURE 6. METAL CURRENT ELECTRODES  
AND POROUS-POT POTENTIAL ELECTRODES USED  
WITH THE EARTH RESISTIVITY INSTRUMENT



Porous-pot electrodes were used as potential electrodes, and metal electrodes were used as current electrodes. Porous-pot electrodes are non-polarizing electrodes used to eliminate problems and errors caused by galvanic action between metal electrodes and the soil.

Electrical contact with the earth using a porous-pot is made through the moist bottom of the pot. The body of the pot is glazed porcelain except for the pottom. Saturated copper sulphate solution inside the pot permeates the porous ceramic bottom to form the electrical ground surface contact. A pure copper electrode immersed in the solution and passing through the cover on the pot permits connection to the instrument.

Pusher style metal electrodes as shown in Figure 6 were used as current electrodes except in rocky areas where electrodes must be driven in. The current electrode assembly is 4 feet (1.2 m) long including a 1-foot (0.3-m) long, 1/2-inch (13-mm) diameter copper clad steel electrode at one end attached to a rod having a horizontal extension that allows an operator to push it into the soil using foot pressure. No ground contact problems were encountered using the metal current electrodes.

The cable reel set shown in Figure 5 provided a convenient means for handling the wire leads used with the current and potential electrodes. This reel assembly contains four reels of vinyl insulated 18 gauge wire, each containing 1000 feet (305 m) of wire. The cable reels are supported in bronze bearings and have hand cranks for rapid rewinding of the wire. Connections to the instrument are made through copper disks mounted on each reel and through heavy carbon brushes contacting the copper disks. The brushes connect to a quick disconnect connector on the outside of the case. Cable reels are insulated from the case. A short jumper cable connects the reel case to the instrument.

## 2. AC Instrument

Alternating current resistivity measurements were also used for two reasons: (1) surveys can be made much faster because there is no requirement to balance out DC earth materials, and (2) the borehole measurements necessarily used metallic potential electrodes which would give rise to galvanic potentials in a DC system.



The AC instrumentation was laboratory constructed and comprised a constant current power source and a high input impedance autoranging voltmeter with digital readout.

The AC current source operated at a frequency of 97 Hz to prevent signal interference from power line frequencies and harmonics. The constant current capability was necessary to prevent electrode contact resistance variations from causing errors.

The input signals to the voltmeter were amplified using a differential amplifier arrangement and narrowband filtered to eliminate noise before it was connected to the voltmeter circuit. The input impedance was in the range of 25 megohms, thus, keeping errors caused by potential electrode contact resistance variations to a minimum.

A great advantage in using AC instrumentation for surface resistivity measurements is faster measurements. With the DC instrument, time is required to first adjust a self potential dial for a null reading and, then, to adjust another dial for a null reading to obtain the desired resistance value. When AC power is used, the polarizing effects around electrodes are eliminated by the current flow reversals. Therefore, since most unwanted ground currents are DC no compensation or nulling adjustment is required. Using an autoranging voltmeter to read potentials, from which resistance is finally calculated, the reading for the measurement can be made immediately after the electrodes are placed in contact with the earth.

Electrodes used with AC instrumentation were all metal. Stainless steel, steel, copper clad steel, and aluminum were all used successfully.

Special spring potential electrodes were fabricated for use in the boreholes. Both beryllium copper and stainless steel were used to construct these electrodes as shown in Figure 7. The electrodes were assembled on a special section of one-inch (25.4-mm) PVC pipe. Additional 10-foot (3-m) sections were fabricated with special end connectors so that the potential measuring pair of electrodes could be lowered by hand to any depth in the borehole.

A short cylindrical aluminum electrode was constructed to be used as a current electrode that could be lowered to the bottom of a borehole to make electrical contact through a small amount of water poured into the hole. The electrode is approximately

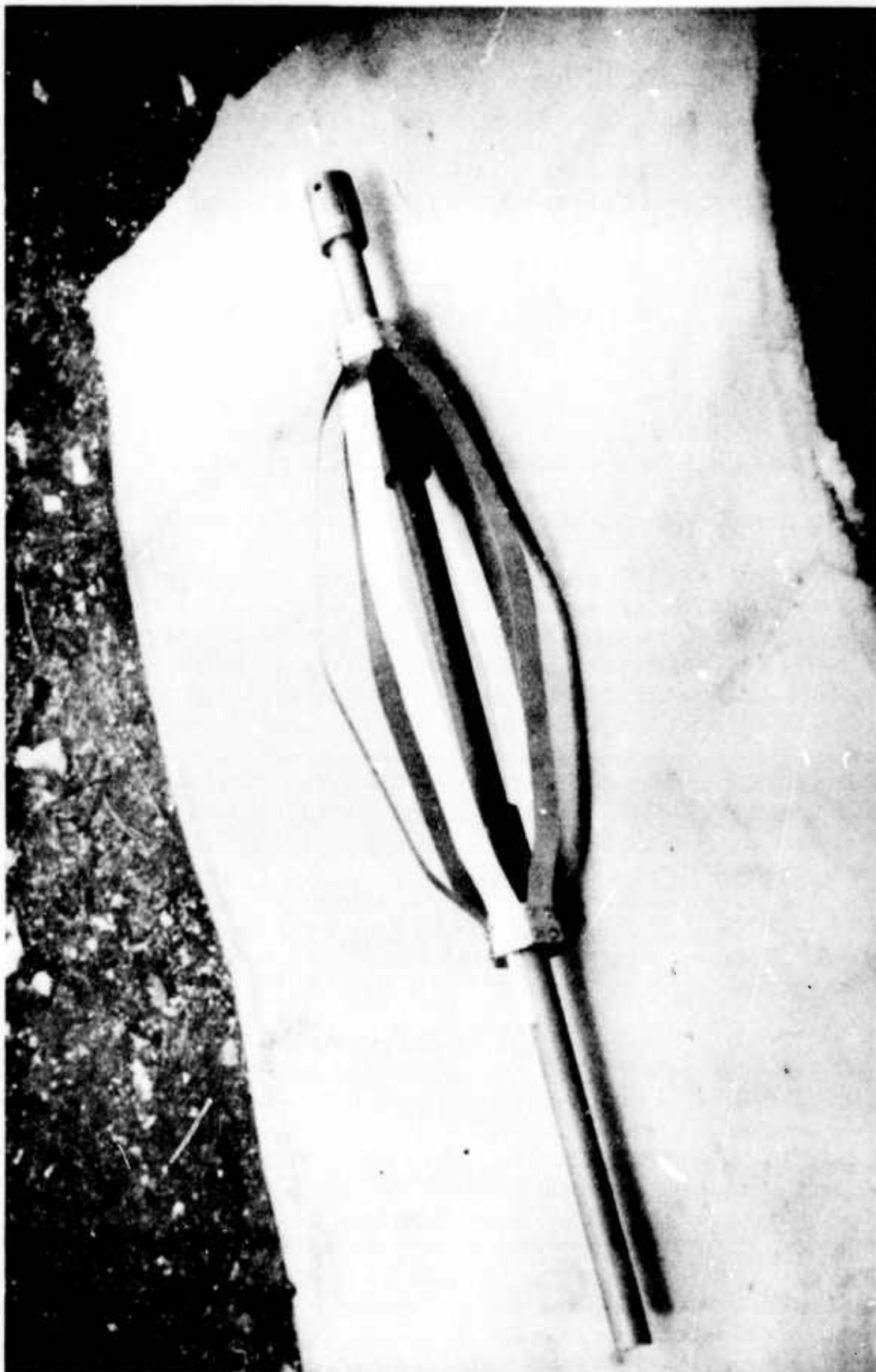


FIGURE 7. PHOTOGRAPH OF A BOREHOLE RESISTIVITY  
POTENTIAL ELECTRODE

8 inches (203 mm) long, 1-1/4 inches (32 mm) in diameter, and weighs 4-1/2 pounds (2 kg). It was made by filling a section of aluminum tubing with lead and attaching an electrical terminal and an eye connection for mechanical attachment for raising and lowering it in a hole.

A special waterproof cable was made up for use with the potential electrodes. It is a Belden 8728 cable with a polyurethane jacket. The cable is 20 feet (6.1 m) long terminated at the electrode end by an encapsulated high-input impedance preamplifier having waterproof leads that attach to the potential electrodes. The other end of the cable connects to a filter amplifier and voltmeter at the ground surface. The cable was made waterproof for anticipated future wet-hole use.

### III. FIELD TESTS

#### A. Idaho Springs, Colorado, Site

##### 1. Site Description

The test site at Idaho Springs, Colorado, was at the Colorado School of Mines Experimental mine. Located at an elevation of about 8000 feet (2.4 km) the mine adit extends into the mountain a distance of about 5 miles (8 km). Its cross section is approximately 10 x 10 feet (3 x 3 m) cut into almost solid granite. The mountain slopes upward from the adit entrance at a 30° angle making it possible to select any desired overburden thickness when field tests are made. The very thin soil is a sandy composite of mostly weathered granite. A good portion of the surface area above the adit is solid rock. Figure 8 is a view of the test site showing the entrance to the adit and the very rough steep slope where resistivity measurements were made. Figure 9 is a photograph showing the sloping area and the type of surface encountered during the tests. Figure 10 is another photograph taken in the area showing the rock that comes up to the surface. The hole is a shaft going into the mine.

##### 2. Site Preparation

The entire area over the mine adit that was to be used in the tests was surveyed, and contour maps were made. This was done to aid in surface resistivity data interpretation and to locate a borehole in the road that was to be used for borehole resistivity measurements. Figure 11 is a contour map of the entire area used, with contour intervals of 20 feet (6.1 m). From this map traverse lines were selected to allow resistivity surveys to be made across the adit where it was 50 and 73 feet (15.2 and 22.2 m) below the surface. Figure 12 is a contour map of the surface from the adit level to the service road that crossed over it at an elevation of 30 feet (9.1 m). The Sections shown on this map indicate sections through a borehole that will be discussed later.

Layout plans included two boreholes to be put into the service road that would miss the adit by distances of 16 and 40 feet (4.9 and 12.2 m). Drilling difficulties prevented completion of one of the holes. Only the one that had a miss-distance of 16 feet (4.9 m) was completed and used in the tests. It was drilled to a depth of 60 feet (18.3 m) which was about 20 feet (6.1 m) deeper than the floor of the adit. Heavy rains after the hole was completed washed about 10 feet

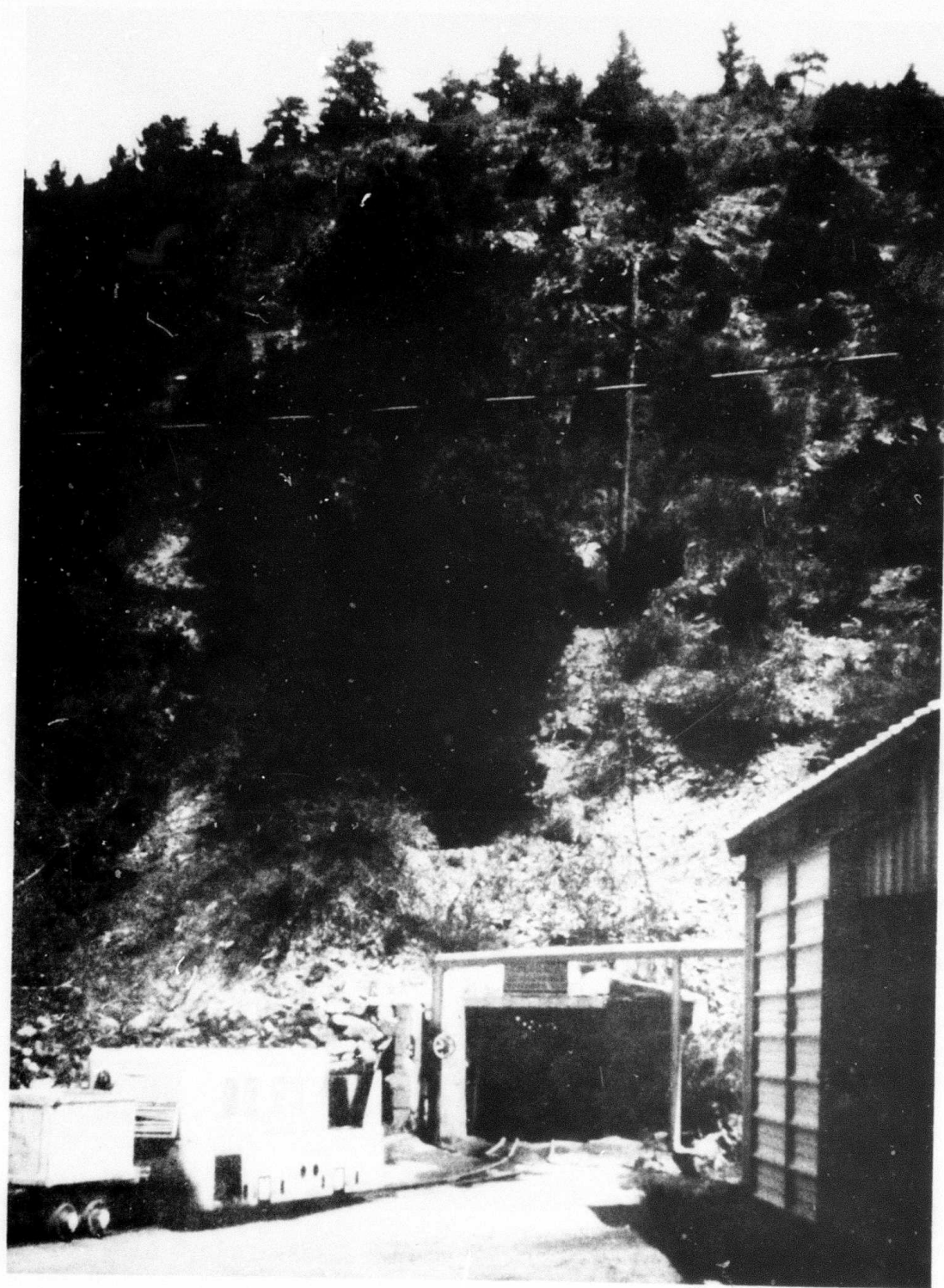


FIGURE 8. VIEW OF THE COLORADO SCHOOL OF MINES  
TEST SITE SHOWING ADIT ENTRANCE





FIGURE 9. VIEW OF THE COLORADO SCHOOL OF MINES  
TEST SITE SHOWING THE RUGGED SURFACE AND STEEP SLOPE



FIGURE 10. VIEW OF MINE SHAFT SHOWING GRANITE OUTCROPPING

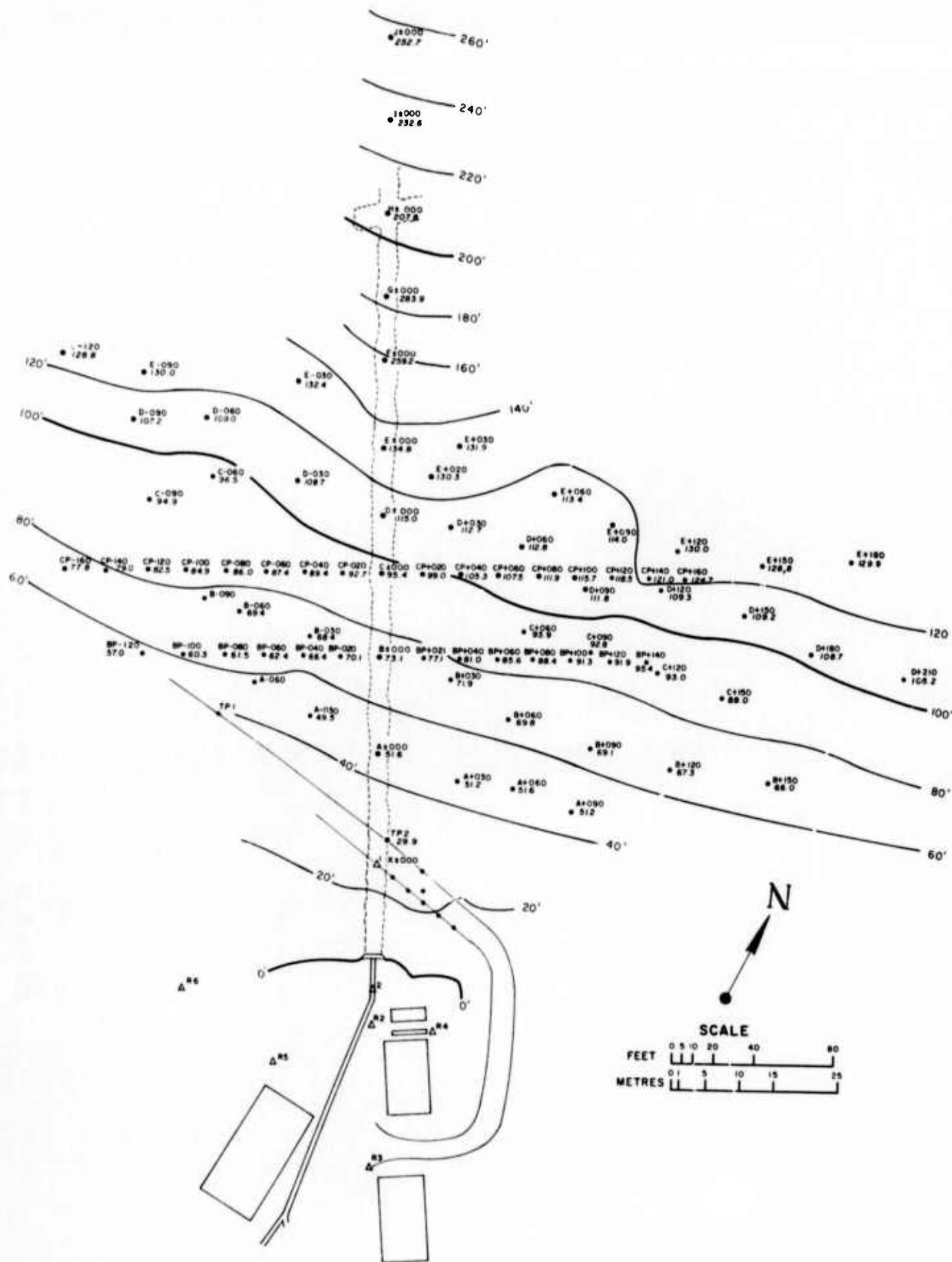


FIGURE 11. CONTOUR MAP OF THE AREA OVER  
THE MINE AT IDAHO SPRINGS, COLORADO

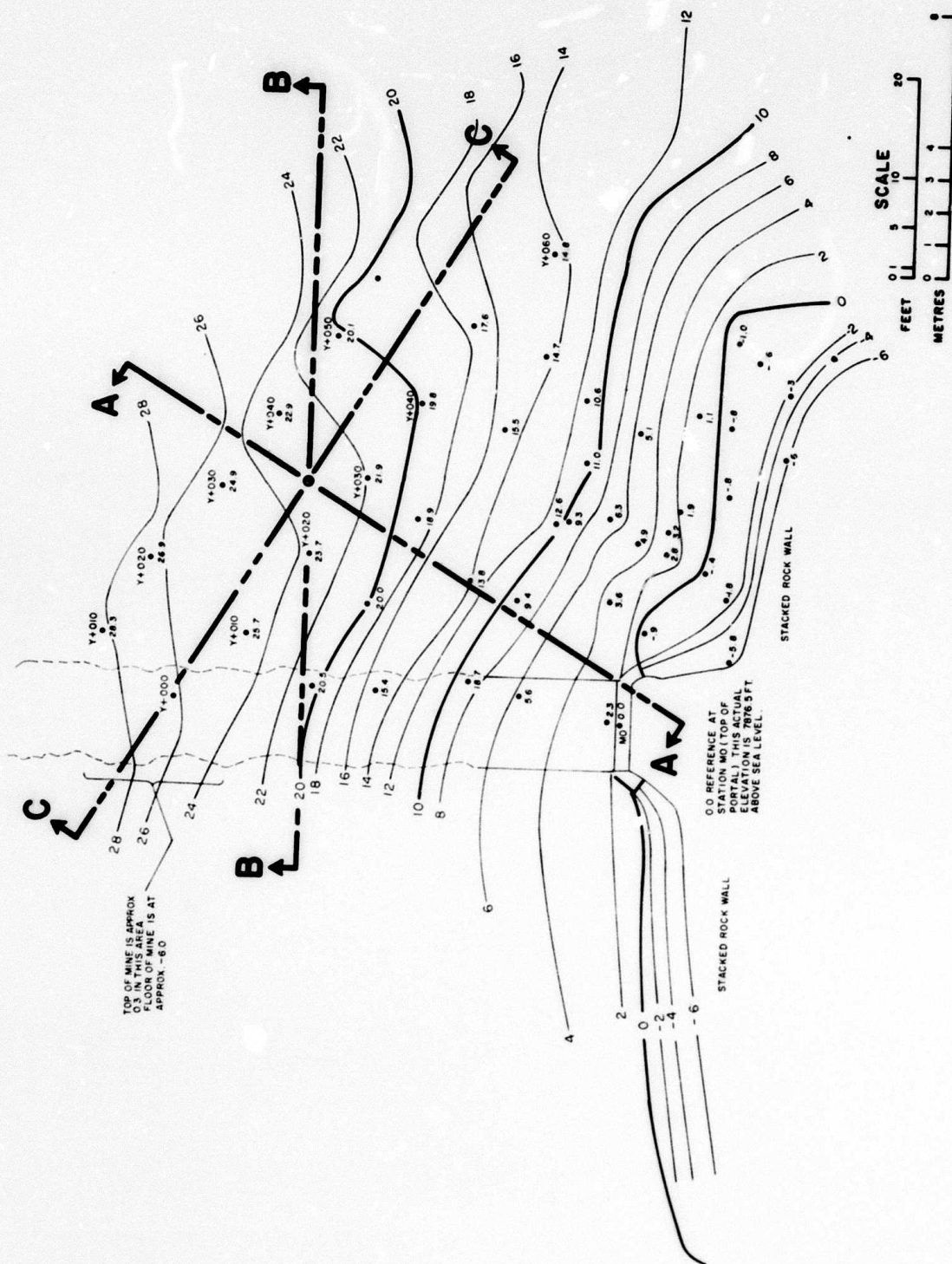


FIGURE 12. CONTOUR MAP OF THE SLOPING SURFACE  
FROM MINE ENTRANCE TO SERVICE ROAD



(3 m) of soil into the hole leaving a working depth of 50 feet (15.2 m).

### 3. Resistivity Surveys and Results

Three resistivity surveys were made crossing the mine adit where overburden thickness was 30, 50 and 73 feet (9.1, 15.2 and 22.2 m). A set of measurements was also made down the single dry borehole.

The pole-dipole electrode array was with both AC- and DC-instrumentation. Potential electrode spacings of both 5 and 10 feet (1.5 and 3 m) were tried. It was generally found that ten-foot (3 m) potential electrode spacing gave good target resolution but the five-foot (1.5 m) spacing caused many smaller anomalies to be detected. Most traverses were run using a fixed potential electrode spacing of 10 feet (3 m) incremented in distance from the current electrode in 5-foot (1.5 m) intervals. The results using AC and DC power were identical. (This comparison was made on the service road traverse only.)

Excellent results were obtained on the road traverse where the adit was 30 feet (9.1 m) below the surface. A total of 4 arc pairs crossed in the volume where the adit was located as shown in Figure 13. The search in this case was made by starting with one current electrode (infinity) 850 feet (259.1 m) from the adit center line and the near current electrode 100 feet (30.5 m) from the center line in the opposite direction (refer to the figure). Starting with the 10-foot-spaced (3-m) potential electrodes at 5 and 15 feet (1.5 and 4.6 m) from the current electrode they were incremented in 5-foot (1.5-m) intervals to the 10- and 20-foot (3- and 6.1-m) marks and so on out to the 65-, 75-foot (19.8-, 22.9-m) locations. The current electrode was then moved closer to the adit center line by an increment of 30 feet (9.1 m), and the traverse repeated on both the forward and reverse sides of the current electrode. The figure shows the locations of other high and low resistivity manifestations near the road surface. The low resistivity areas labeled "A" and "C" were known moist areas. The high resistivity anomalies were caused by near surface and actual outcroppings of granite.

Construction of the graphical sketch in Figure 13 was done as was shown earlier in Figure 3 by observing the graphs of measured data for high and/or low resistivity indications. These were then labeled and their locations transferred to a graphical sketch sheet where the bearing arcs were drawn.



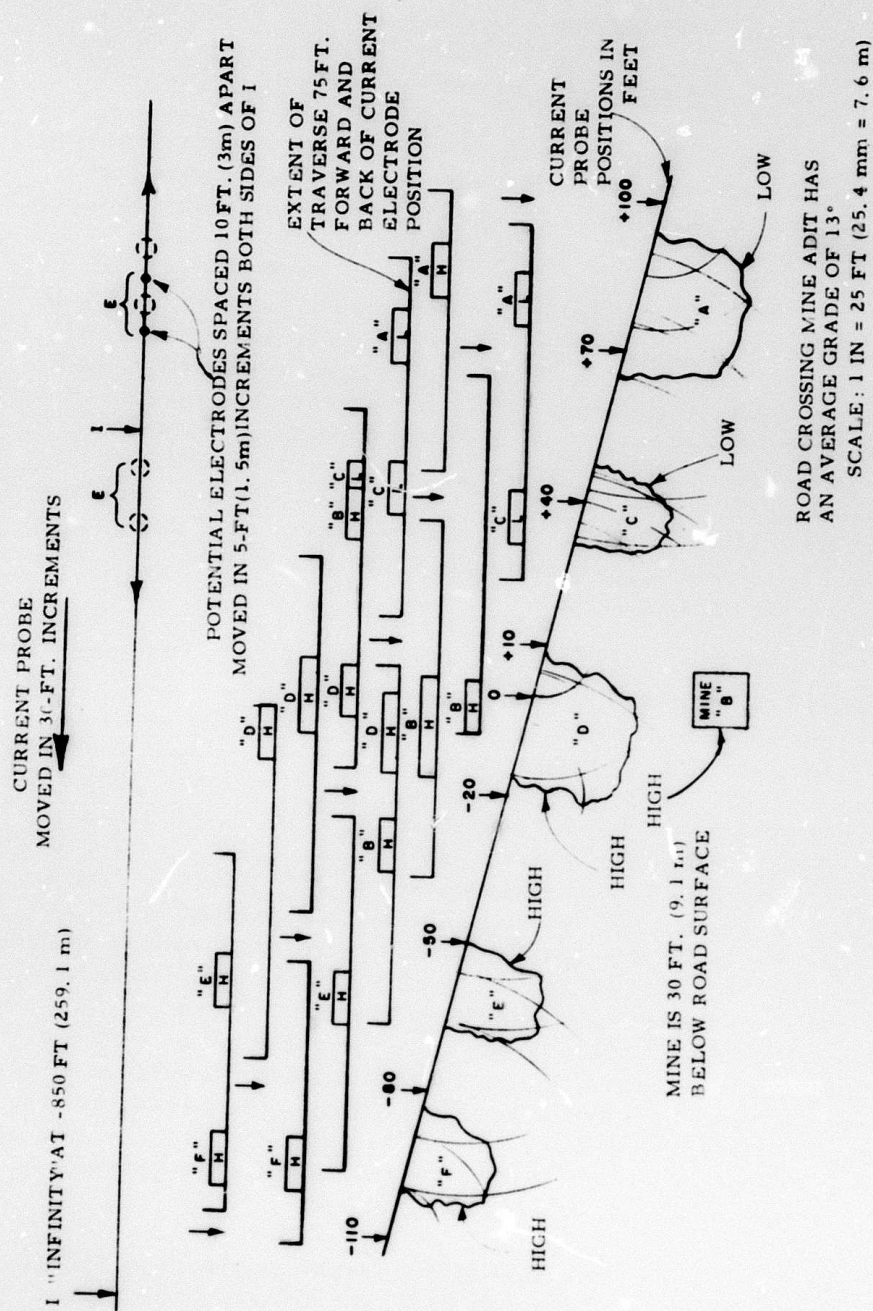


FIGURE 13. GRAPHICAL POLE-DIPOLE RESISTIVITY SURVEY RESULTS  
FOR TRAVERSE ALONG SERVICE ROAD CROSSING MINE ADIT  
(Colorado School of Mines Experimental Mine)

Interpretation of the data taken over the rough broken rock terrain is difficult. Ground surface effects are very strong, and in many cases they almost mask the anomaly caused by the mine adit. However, careful observation of ground surface topography aids in eliminating many of these effects from the data graphs. Figure 14 shows the interpreted results of a traverse along survey line A where overburden was 50 feet (15.2 m) thick. At least six arcs representing resistivity highs intersect in the volume of rock where the mine adit is located. Also, as shown, approximate soil depth variations could be determined along with near surface rock. Other below surface anomalies were not verified, but the low resistivity volume seen near the mine is most likely caused by water. There was seepage into the mine in this area.

The results of a traverse that crossed over the mine adit where it was 73 feet (22.2 m) below the surface were not as outstanding. Detection results of the traverse along survey line B are shown in Figure 15. There were high resistivity anomalies noted at locations that fitted the target location; but a great number of high resistivity anomalies (as large or larger than the mine anomalies) not associated with the mine adit were detected. Most of these "highs" were surface related effects from observed granite outcropping. On this traverse measurements were made to a distance of 130 feet (39.6 m) each side of the current electrode, and the current electrode was incremented in 40-foot (12.2 m) intervals. The surface anomalies generally appear on the graphs of three consecutive traverses, have about the same shape, and are offset from curve to curve by a distance of 40 feet (12.2 m). If arcs are drawn representing these "highs" they will intersect at the ground surface. "Highs" were located such that there were arc intersections at the mine location. Near-surface resistivity anomaly interpretations are not shown in the Figure 15 sketch.

Resistivity measurements in the borehole gave very definite detection indications. Measurements were made with the current source electrode first at the top of the hole and then at the bottom of the hole. Both 5- and 10-foot (1.5- and 3-m) potential electrode spacings were used. The anomaly appeared larger with the 5-foot (1.5-m) electrode spacing.

Data interpretation results are shown in Figure 16. Three sectional views are shown so that any effects of the surface slopes could be noted. The hole was drilled normal to the plane of the road surface. Because of the slope of the road, the borehole had an angle that was 13° from vertical and also angled slightly in toward the mountain.



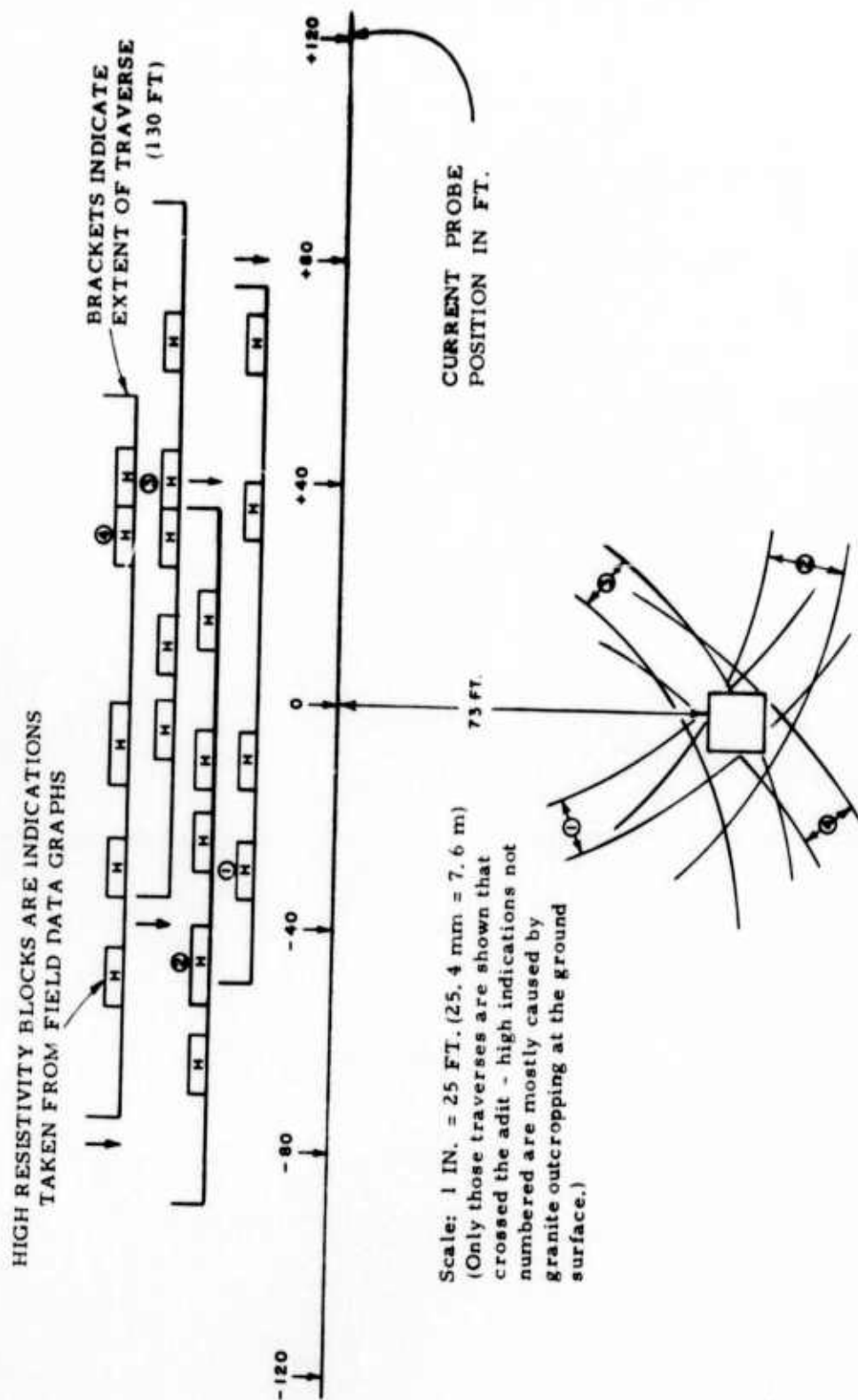


FIGURE 15. GRAPHICAL POLE-DIPOLE RESISTIVITY SURVEY RESULTS FOR  
TRAVERSE ALONG ROW "B" PERPENDICULAR TO MINE ADIT CENTER LINE  
(Colorado School of Mines Experimental Mine)

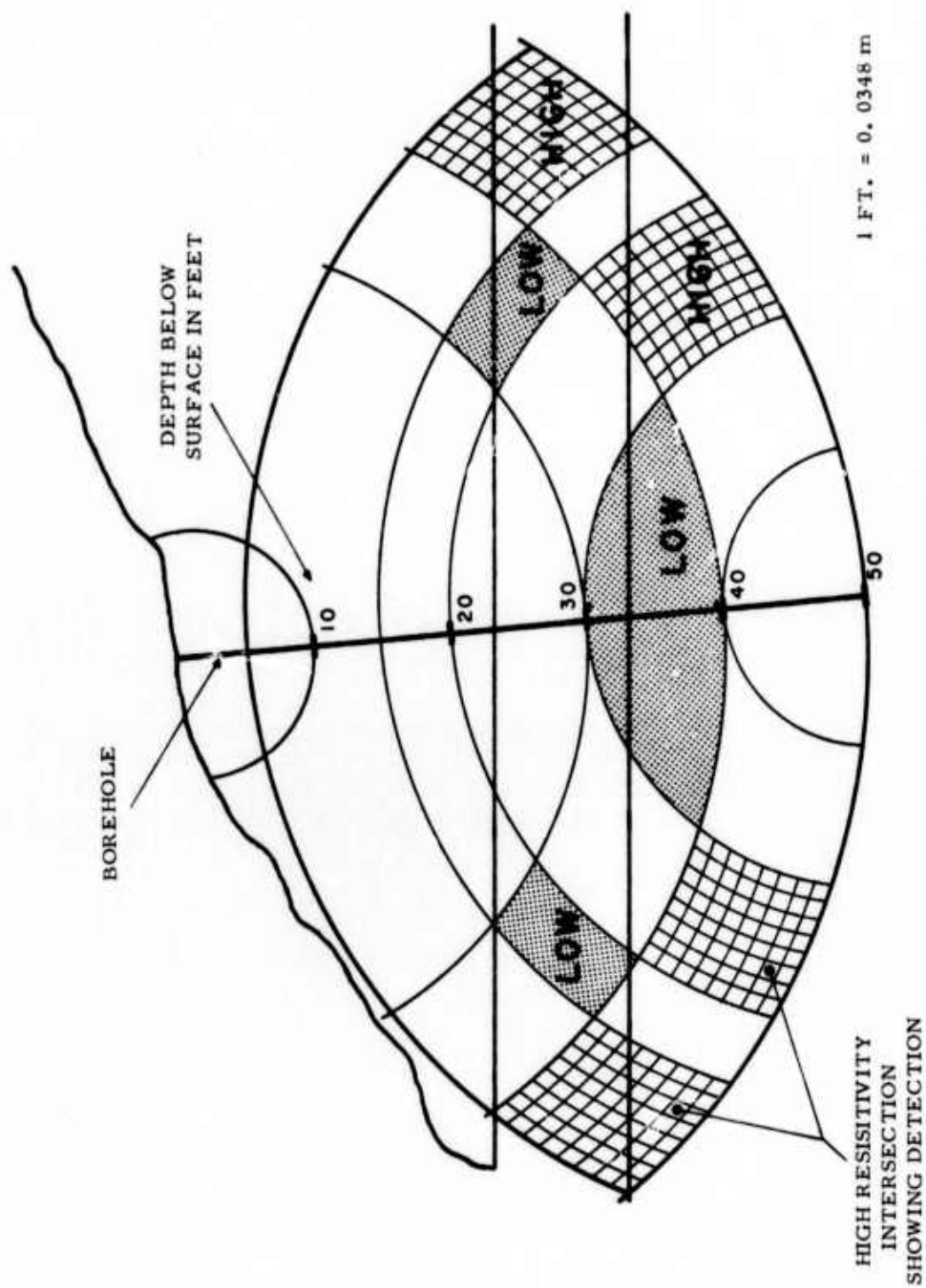
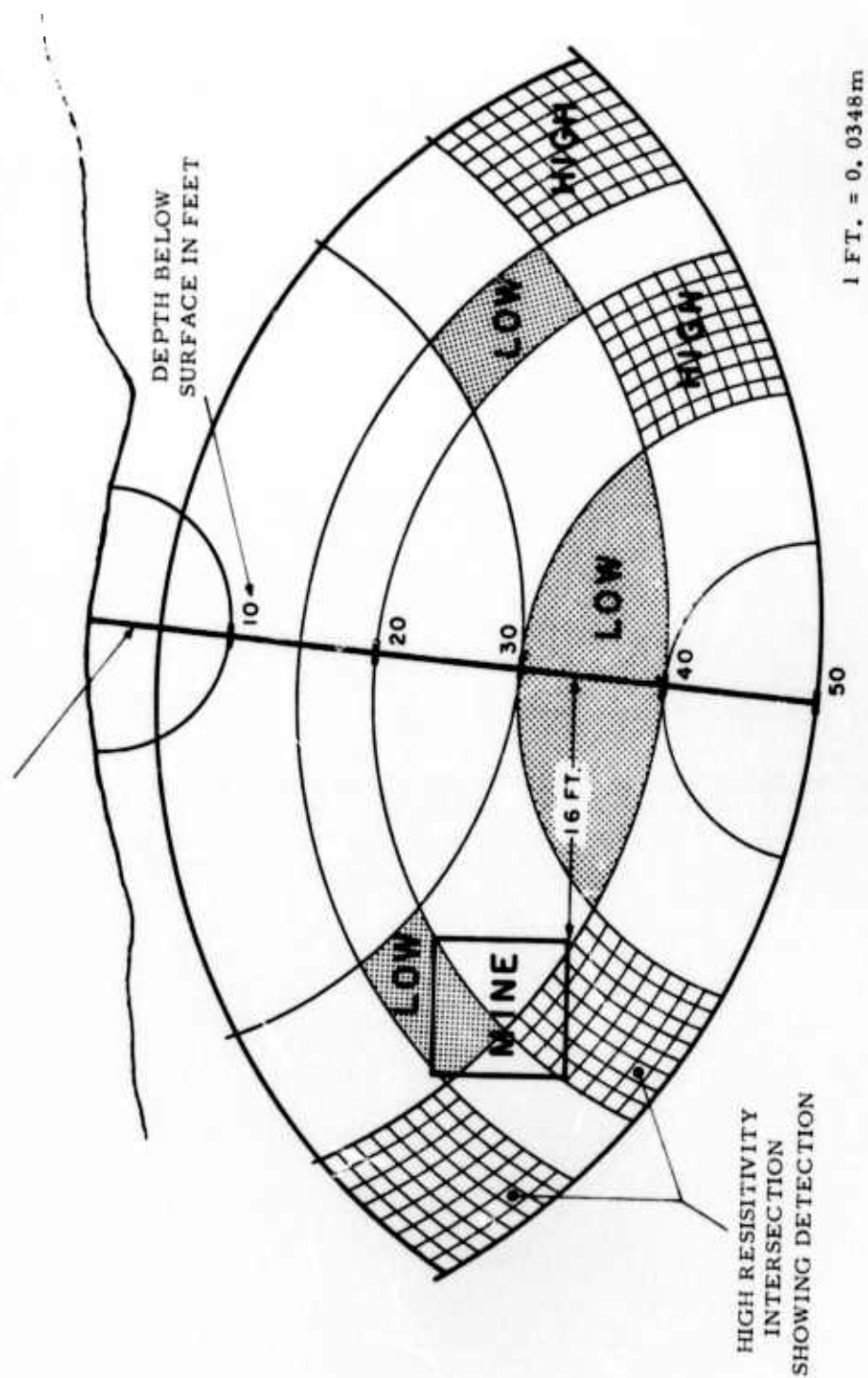


FIGURE 16. SECTIONAL VIEWS OF BOREHOLE DETECTION RESULTS, IDAHO SPRINGS, COLORADO





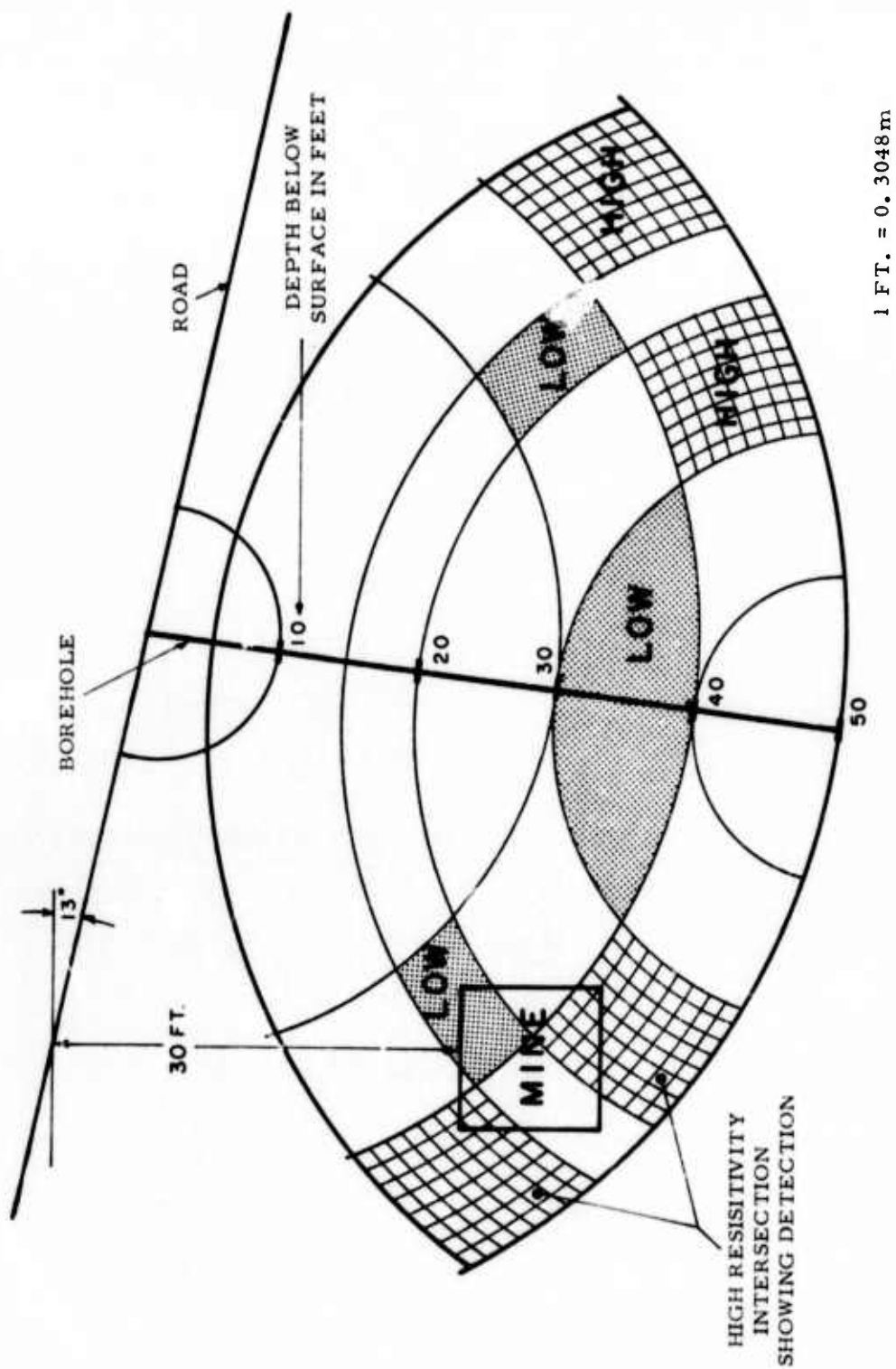


FIGURE 16 (cont.) SECTIONAL VIEWS OF  
BOREHOLE DETECTION RESULTS, IDAHO SPRINGS, COLORADO

Figure 16 (a), Section A, is a plane through the borehole perpendicular to the service road (see Figure 12 for Sectional locations). This particular section provides a view of the maximum surface slope that might affect resistivity measurements. In this view the mine adit appears horizontal running from left to right on the page. Detection results are shown in the figure. The locations pointed out are high resistivity arc crossings that are in the correct location to be caused by the mine. The two marked high resistivity arc crossings at the right of the page are sections of the same potential shells as those shown at the left of the page. It must be remembered that when the current source is below the ground surface, the equipotential shells around it are spherical in shape if the medium is homogeneous. Homogeneous subsurface conditions were assumed throughout these tests. Detection from at least three holes is necessary to obtain an absolute location of the detected target.

The high resistivity anomaly caused by the mine adit was partially countered by the low resistivity anomalies shown. Had these not been encountered the entire volume around the mine would have appeared as high resistivity indications. The low resistivity indication surrounding the borehole at the 30- to 40-foot (9.1- to 12.2-m) depth was caused by water. Water was found at this depth when the hole was drilled; however, it drained before the measurements were made.

This sectional view shows that the surface slope did not affect the arcs that indicated detection. Had they crossed the surface the high resistivity indication would have been questionable. The surface effects on equipotential arcs centered at the top of the borehole are taken care of in the geometrical factor used in calculating apparent resistivity.

Figure 16 (b) is Section B which is a plane through the borehole and perpendicular to the adit center line. This view shows the true distance from the borehole to the adit. The slope of the ground surface in this direction is seen to be relatively flat compared to that shown in Figure 16 (a). The resistivity high anomalies can be seen around the mine in this view. Otherwise the results appear the same as in Figure 16 (a).

Figure 16 (c) is a sectional view of a plane passing through the borehole and parallel to the service road centerline. Again, it can be seen that the surface slope is not interfering with the potential shells that show resistivity anomalies.

In summary, the mine adit was detected from resistivity measurements made in a borehole that passed the adit at a distance of 16 feet (4.9 m). Best results were obtained when the potential electrode spacing in the pole-dipole electrode array was 5 feet (1.5 m).

B. Gold Hill, Colorado, Site

1. Site Description

The town of Gold Hill, Colorado, is located approximately 15 miles (24 km) northwest of Boulder. The Gold Hill test site is located about one mile (1.6 km) west of the town at an elevation of 8500 feet (2.6 km). It is the site of an abandoned mine that has an adit that runs through the mountain a distance of approximately 600 feet (183 m). The cross section of the passage is about 5 x 6 feet (1.5 x 1.8 m). The ground surface has an average upward slope from the adit entrance of 23°. The ground surface is covered mostly with grass and large pine trees. There is very little brush to interfere with surface surveys. The subsurface structure is granite overlain by a sandy mixture of mostly weathered granite. A large amount of quartz is scattered over the ground surface. Figure 17 is a view of the area looking southeast along survey line Number Three where one resistivity search traverse was made. The mountain in the background was the location of the infinity current electrode.

Two faults ran through the test area almost parallel and about 150 feet (45.7 m) apart. Resistivity survey traverse lines crossed these fault lines in several places. Mining had been done along these faults leaving craters of various sizes along the way. They averaged about 30 feet (9.1 m) in diameter with depths of about 20 feet (6.1 m) to the partially filled in bottom. Figure 18 is a view of a typical crater.

Comparing the Gold Hill test site to the Colorado School of Mines site, the Gold Hill site was less rugged, and slopes were not as steep. It also had more top soil making electrode placement easier. The many craters at Gold Hill caused resistivity anomalies when a traverse came near one, but these were identifiable when the data were processed. Overall, the Gold Hill site was more accessible and easier to work.



FIGURE 17. PHOTOGRAPH OF GOLD HILL TEST SITE  
LOOKING SOUTHEAST ALONG SURVEY LINE 3





FIGURE 18. VIEW SHOWING A LARGE CRATER NEAR  
RESISTIVITY TRAVERSE LINES AT THE GOLD HILL,  
COLORADO, TEST SITE

## 2. Site Preparation

The only site preparation necessary was to drill holes for borehole testing. The United States Bureau of Mines in Denver, Colorado, had an interest in the results of the tests to be done at the Gold Hill site. They had used the site for some of their experiments and obtained permission for work on this program to be done there. Survey lines were already staked from their previous work, and these were useable for the resistivity surveys. The Bureau of Mines also needed boreholes for their tests. They performed the drilling and allowed the holes to be used for tests on this program.

Two boreholes were planned: one 25 feet (7.6 m) from the adit center line and one 50 feet (15.2 m) from the center line. These were to be drilled at a location where there was about 80 feet (24.4 m) of overburden and drilled to a depth of 160 feet (48.8 m). After a great deal of equipment trouble, one hole 3 inches (76.2 mm) in diameter was completed to a depth of 135 feet (41.2 m) by the time the field measurements had to be completed. Both holes were finally completed to 160 feet (48.8 m) but too late to be used in the current program.

## 3. Resistivity Surveys and Results

Figure 19 is a topographical sketch of the test area. The adit runs from the road level, Hazel A Portal, into the mountain (bottom of the page to the top). The Bureau of Mines survey lines numbered 3, 4, and 7 are shown crossing the adit. The borehole locations are shown on Line 7. Overburden under Line 3 was 30 feet (9.1 m); under Line 4, 47 feet (14.3 m); and under Line 7, 81 feet (24.7 m). Resistivity traverses were made along these lines and down the one partially completed borehole.

Using potential electrode spacing of 5 feet (1.5 m) incremented in 5-foot (1.5-m) intervals the mine adit was detected on all three surface traverses. Not only was the adit detected, but all known surface features could be distinguished by their resistivity anomalies. An example of detection results using the graphical construction method is shown in Figure 20. The traverse shown is along Line 7 on the topographic map (see Figure 19). The map shows two rather large patches of granite outcropping starting about 60 feet (18.3 m) to the right of the adit center line. Also, two fault lines cross the traverse. As can be seen on the resistivity data sketch, Figure 20, there are large concentrations of high resistivity indications at both granite outcrop locations. Also noted are strong low resistivity indications where the faults were crossed (arcs not drawn in purposely to reduce clutter).

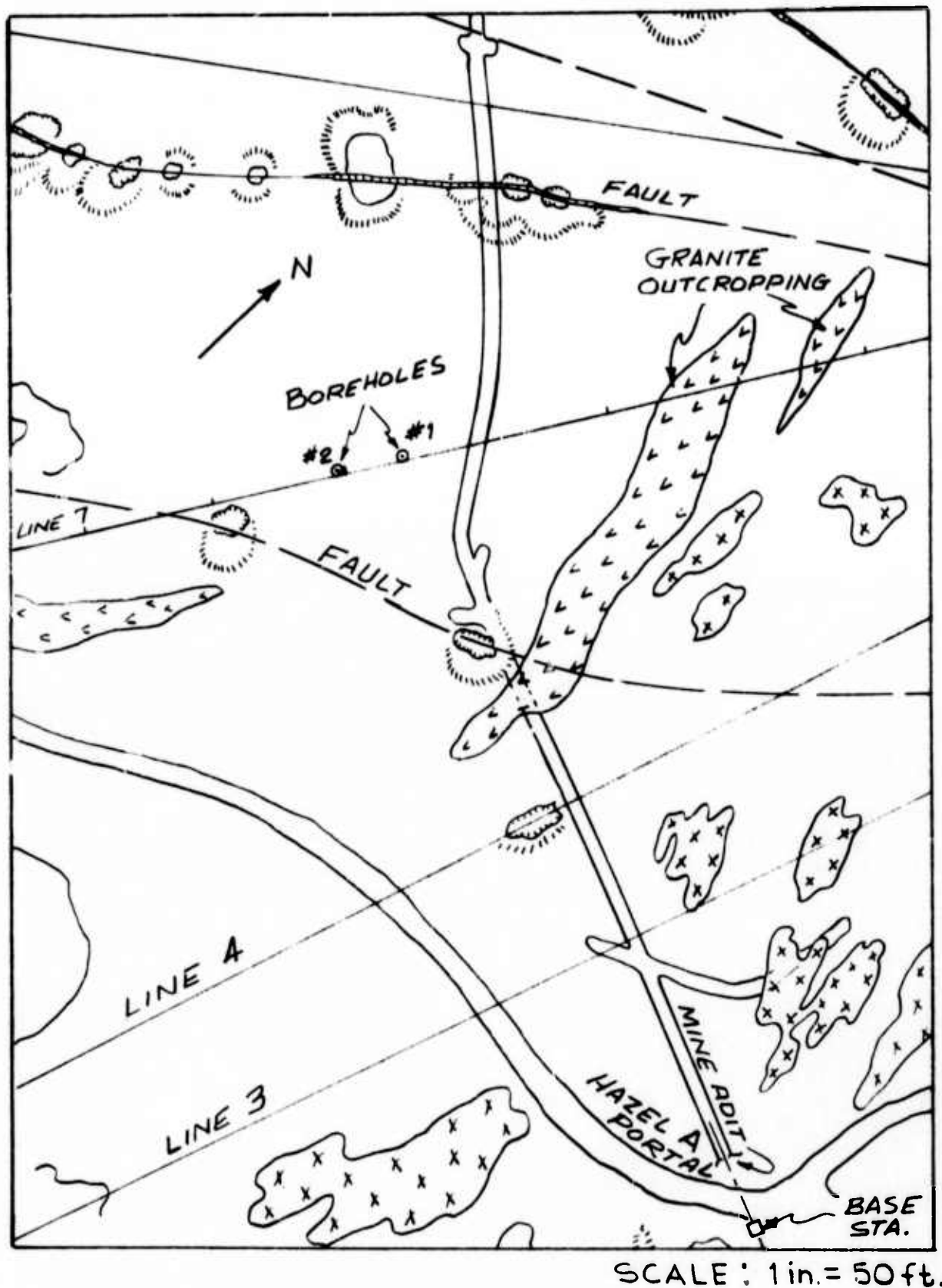
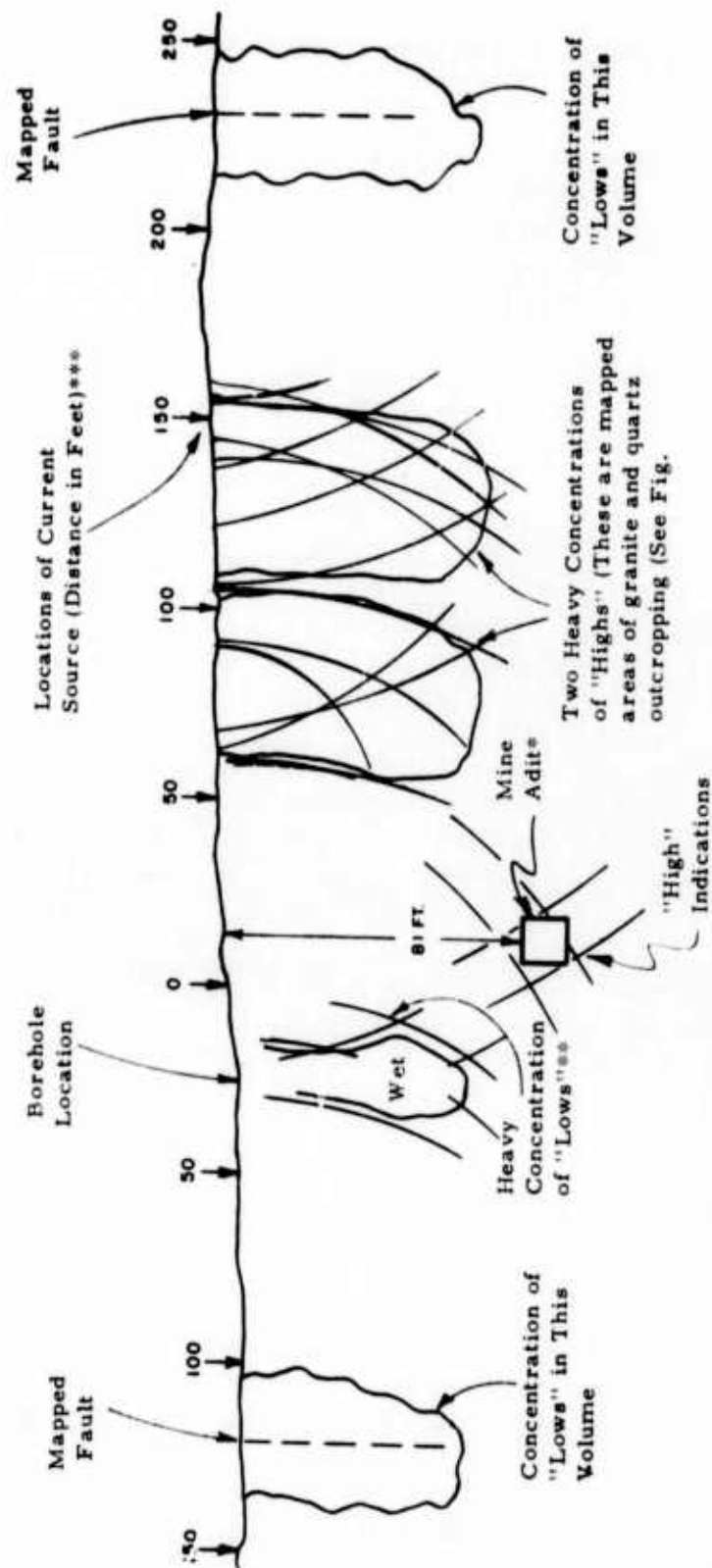


FIGURE 19. TOPOGRAPHICAL MAP OF THE  
GOLD HILL, COLORADO, TEST AREA



NOTE: Only parts of arcs are shown that contribute to or outline major features.

\* 6 arc pairs crossed at adit location

\*\* 8 arc pairs crossed in the wet location of the borehole

\*\*\* 1 FT. = 0.3048 m

FIGURE 20. SKETCH OF EARTH RESISTIVITY INTERPRETATION OF A TRAVERSE ALONG SURVEY LINE 7, GOLD HILL, COLORADO

The "lows" were probably caused by moisture concentration and other conducting materials in the faults.

The mine adit showed up very clearly even at the 81-foot (24.7-m) depth. Six arc pairs crossed at the adit location. An interesting detection result is the detection of the subsurface water in the volume of earth where the hole was bored. This was a very positive indication with 8 arc pairs crossing in that location.

Figures 21 and 22 are included to provide an example of the data plots from which the interpretation in Figure 20 was made. On each sheet the current source electrode positions are marked on the horizontal line labeled SURFACE. The curves immediately to the left and right of each current electrode position are the data curves plotted from traverses run to the left and right of that current electrode position. The traverses on which these data were taken were nominally 200 feet (61 m) on each side of the current electrode. In some cases when the traverse was directed away from the adit, the traverse was shorter. In other cases the traverse length was extended to ascertain that it crossed the adit far enough to allow detection.

Only the anomalies caused by the adit are labeled. These were determined when the data were studied and analyzed. The small size of the mine anomaly compared to other anomalies will be noted. On analyzing the data, it will be found that most of the large anomalies are caused by near surface rock outcropping or by craters near the traverse line. It must be remembered that the potential bowls or resistivity shells around the current electrode are shells somewhat hemispherical in shape (hemispherical in a homogeneous medium), and resistivity anomalies within several feet of a traverse line will be detected.

Detection of the adit under 30 feet (9.1 m) of overburden was definite. At the 47-foot (14.3-m) overburden location, detection indications were strong; but a crater only a few feet southwest of the adit center line (refer to Figure 19) on this traverse confused the results, because data arcs passing through the adit also passed through the crater. Anyone interpreting the data from that location not knowing the adit was below would have misinterpreted the results as being caused by the crater.

Borehole resistivity measurements were mostly unsuccessful. The borehole had hit water at a depth of 40 feet (12.2 m) and remained full to that level. It was pumped dry but continued to refill too fast to allow measurements to be made in a dry hole. Since



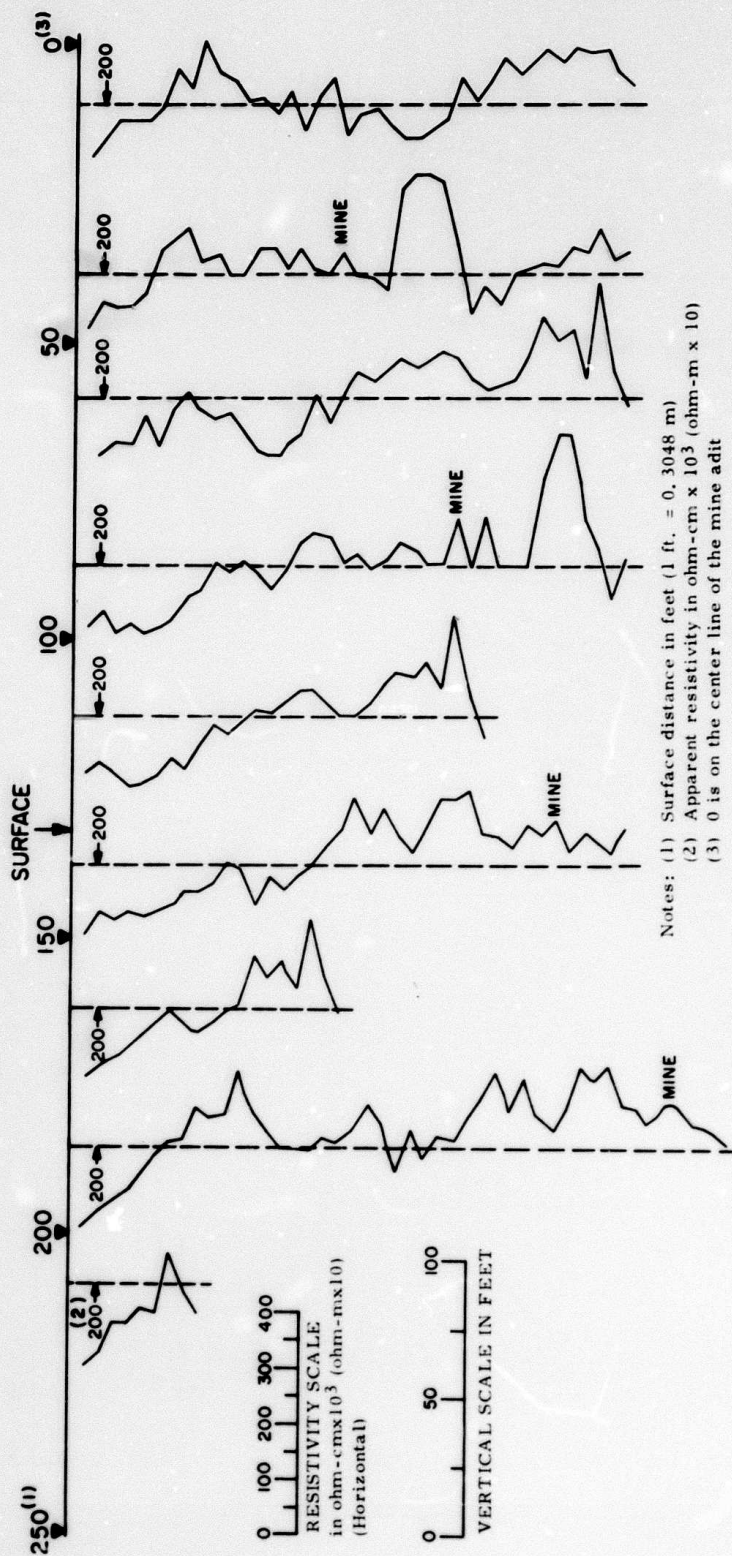


FIGURE 21. RESISTIVITY DATA GRAPHS OF THE SOUTHWEST END OF LINE 7 TRAVERSE, GOLD HILL, COLORADO

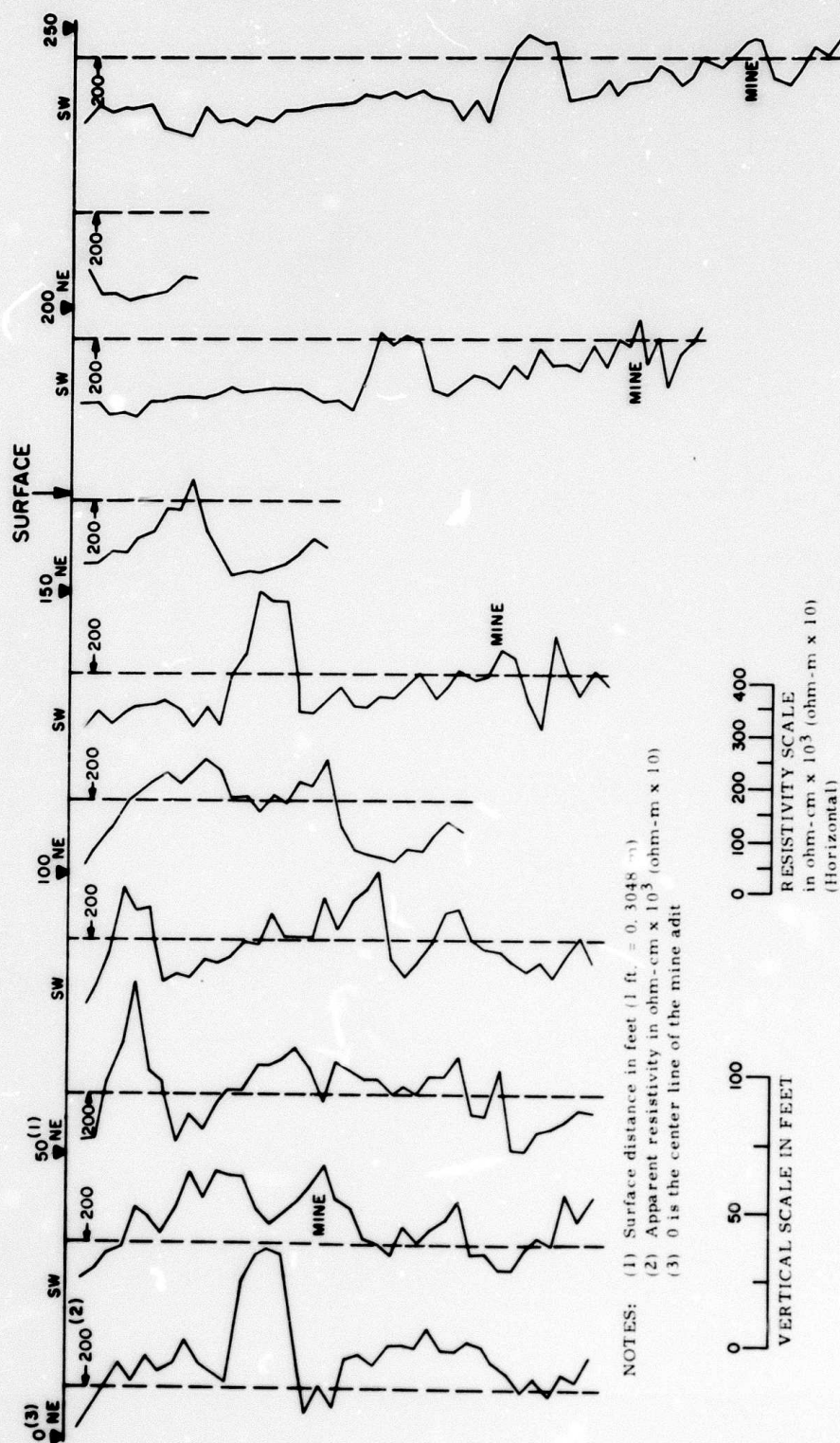


FIGURE 22. RESISTIVITY DATA GRAPHS OF THE NORTH EAST END OF LINE 7 TRAVERSE, GOLD HILL, COLORADO

it could not be kept dry, it was kept full of water to the ground surface so that all measurements would be made in water. The cable and electronics used in the borehole were waterproof and caused no problem. The main problem encountered was the low resistance of the water in the hole that practically shorted the potential electrodes.

Contact with the walls of the hole was also a problem. In drilling this hole, the driller used heavy coats of thick cup grease on all drill rods that were put into the hole to relieve wall friction on the drill rod and make drilling easier. This left a very heavy coat of grease that has a high electrical resistivity on the walls of the hole. The potential electrodes had been designed to slide easily into a dry hole. The net result was bad electrical contact with the walls of the hole and a liquid filled hole that tended to act like a short between electrodes.

The data from the borehole measurements showed one indication of detection, but it was not positive because there was no other overlapping data to actually prove detection. There was one resistivity high that occurred at the correct distance from the current electrode.

The time and funds available did not permit an additional trip to the site in which techniques for performing resistivity surveys in water-filled holes could have been applied.



#### IV. CONCLUSIONS

The objective of the program discussed in this report was to experimentally evaluate earth resistivity profiling as a method of detecting subsurface voids in a granite environment. The resistivity method used a high-resolution electrode array known as a pole-dipole or three-electrode array. Although the program scope was limited, a number of conclusions were reached as follows:

1. Small tunnels with cross sections in the range 6 x 6 feet (1.8 x 1.8 m) can be detected at depths below the ground surface of over 80 feet (24.4 m). The maximum depth was not determined, but probably about 100 feet (30.5 m) would be the limit for such small tunnels with the electrode arrays that were evaluated.
2. Mountainous terrain with varying slopes of over 30° does not appear to affect detection capabilities.
3. Topographical variations such as rock outcropping, variable soil depth, faults, and other features can make data interpretation very complex; but in most cases the resolution of the detection method allows these features to be mapped.
4. The method is most sensitive to near-surface resistivity variations.
5. The larger the potential electrode spacing the less sensitive the method seems to local resistivity variations; also, the smaller the spacing with respect to the diameter of the subsurface target the larger the detection indication. Therefore, the optimum potential electrode spacing would be large enough to eliminate as much background variation (noise) as possible but small enough to enhance target detection capability. A spacing no smaller than one half to one diameter of the suspected target should be an appropriate compromise.
6. Subsurface profiling using the three-electrode resistivity array as described in this report, is a time consuming process. A two-man crew can complete a single 200-foot (61-m) survey traverse in about 15 minutes; however, the required redundancy in this type of measurement will increase the time in the field. A two-man crew can average one 500-foot (152.4 m) survey traverse in an 8-hour day.

7. Drilling is the only known method to absolutely determine the existence of air- or solution-filled subsurface cavities. Resistivity measurements can greatly minimize the required number of boreholes in an area by identifying anomalous areas that could be cavities or tunnels.

8. The three electrode resistivity measurement method of cavity detection can be used in boreholes. Although this arrangement had a very limited test on this program, a mine adit having a cross section of about 10 x 10 feet (3 x 3 m) was detected from a dry borehole 16 feet (4.9 m) away. It is probable that such detection could be made from hole distances of up to 40 feet (12.2 m). This use shows promise, but for better understanding and detection range prediction, both theoretical and experimental studies should be continued.

There are two great advantages to making measurements in a borehole: (1) the rock environment near the electrodes should be much more homogeneous than found near the ground surface, thus eliminating a great deal of "lithological noise" and enhancing the desired anomaly indication; (2) if the target tunnel is very deep, a borehole can put the electrodes within the detection range of the search method.



## V. RECOMMENDATIONS

The three-electrode resistivity method of detecting underground cavities and tunnels has been proven successful in several environments. It has detected voids at depths of over 80 feet (24.4 m) and has worked through sandy loam soil over limestone, sand over limestone, moist clay over dolomite, and through granite. Sometimes detection was very good, and other times it was marginal. Several recommendations to improve detection results can be made based on these field results. These are listed as follows:

### A. Additional Experiments and Studies

Specific experiments and analyses should be performed for the following purposes: (a) to determine the ultimate spatial resolution that can be obtained; (b) to determine the effective volume of earth material and field of view affecting the measurements along a survey path; (c) to improve or develop better methods of field data interpretation; and (d) to study other electrode arrangements that might enhance tunnel anomaly indications.

It was stated by both Bates<sup>4</sup> and Bristow<sup>5</sup> that, when using the pole-dipole electrode array in the manner reported herein, the volume of earth material affecting the potential measurements does not include all of the material implied by the circular arcs used in the analysis. Only a sector of the graphical hemispherical potential shells not greater than about  $\pm 25$  degrees on each side of the traverse line is thought to contribute to the measurement. Results obtained on this program have roughly validated this limit although no detailed studies were possible. This is a very important operational and interpretation feature and should be studied by laboratory modeling of resistivity measurements in a brine tank or other suitable medium, by additional field tests over known subsurface targets, and by theoretical analysis. The same study program could be used to determine the best spatial resolution and usable detection depth realizable with the method.

Detailed interpretation of the resistivity data as collected in practice is often complex and difficult. An in-depth study could lead

---

<sup>4</sup> Bates, loc. cit.

<sup>5</sup> Bristow, loc. cit.

to improved graphical analysis and, possibly, by computer processing, to automatic data reduction and subsurface mapping.

Other field data collection methods might be used that would take advantage of the physical shape of a tunnel. Since the tunnel can be visualized as a long cylinder, an electrode array could probably be used that would take advantage of that shape. Line arrays could be laid out and measurements made in the same manner as was described for the standard pole-dipole measurement. For example, a current electrode in the form of a wire 100 feet (30.5 m) long could be laid out parallel to a suspected tunnel axis and staked to the ground at several points. Potential electrodes of the same form would then be used to make potential measurements. Such an array should have a signal averaging effect that would enhance the tunnel anomaly and reduce near surface clutter not common to the entire length of the line electrodes.

Other electrode arrays such as a dipole-dipole array should also be investigated.

B. Study the Resistivity Contrasts Between Earth Materials Associated With Cavity Detection

The size of the resistivity anomaly that a given subsurface target will cause can only be derived if the resistivities of the various materials are known. Samples of soil, bedrock, and water-soil mixtures from water- and mud-filled cavities should be collected from areas of interest and their electrical and electromagnetic properties measured and analyzed. A great deal of information is available on electrical properties of rock, but more data are needed on those materials covering and in the vicinity of the rock.

C. Develop State-of-the-Art AC Resistivity Instrumentation

Ground current variations during the course of a survey traverse can cause errors that appear to be resistivity anomalies when the data are analyzed. A temperature stable constant-current power source should be developed to work in a wide range of ambient temperatures and that can supply ground currents under very dry soil conditions. It should be capable of supplying a constant current of at least 10 ma when combined earth resistance and electrode contact resistance is as high as 50,000 ohms.

The voltmeter section of the instrumentation should be built to have a very high input impedance, in the range of 10 megohms, to prevent potential measurement errors that might be caused by high electrode contact resistance. A low impedance meter across the potential electrodes would allow current to flow in a circuit through the meter, the electrode contact resistance, and the earth, causing a potential drop across any electrode contact resistance. This would produce an error voltage which might be interpreted as measured earth potential. Such features as narrow-band synchronous detection should be built into the meter input circuit to give best possible signal-to-noise ratio. To aid in making field measurements as fast as possible, an autoranging voltmeter should be used with a digital readout. Another feature that should be added especially for borehole operation is a recorder output so that continuous data could be recorded as electrodes were moved up and down the borehole walls.

D. Develop a Mobile, Rolling-Contact-Electrode Earth Resistivity Survey System

It is recommended that an earth resistivity system be developed that would allow continuous measurements using a pole-dipole electrode arrangement in which the electrodes are pulled along the ground surface using a small tractor-type vehicle. Automatic data acquisition and processing could readily be built into such a system to provide direct graphical printouts or other displays of apparent resistivity variations and depth profiles as the electrodes move along a selected traverse. With digital data processing the graphical analysis as described for manual data reduction could provide near real time output information and hardcopy maps delineating the locations, depths and sizes of the detected underground cavities.

Another version of continuous measurements for terrain where a vehicle cannot travel would be a system whereby current electrodes are placed as usual, but the potential electrodes are rolling types. Using an electrode spacing of about 5 feet (1.5 m) it is conceivable that a rolling-contact array comprising only the two potential electrodes could be built that could be pushed or pulled along the ground surface by a man where the terrain would allow. The output from the array could be continuously recorded for later interpretation. The ability to measure earth resistivity using rolling electrodes was demonstrated in 1972 by SwRI<sup>6</sup>.

---

<sup>6</sup> L. S. Fountain, "An Exploratory Study of Soil Resistivity Measurements Using a Rolling Contact Electrode Array," Final Technical Report, SwRI Internal Research Project 14-9057, April 1972.

E. Continue the Investigation of Resistivity  
Borehole Techniques

This would require the development of better borehole electrodes, collection of much more field data in areas of known targets such as mine adits or caves, and solving the problem of making measurements in a liquid-filled hole.

F. Undertake the Long-Range Development of a State-of-the-Art Ground Penetrating Radar for Tunnel Search Applications

Radar tests have shown very good possibilities for the method.<sup>7</sup> The main problems encountered in the field have been penetration depth and small target detection and resolution. Radar technology is presently available to permit the development of a ground penetrating radar system having significantly improved performance over any that are presently in use. The detection depth capabilities could be expanded greatly by increasing transmitter power, by improving receiver design, and by incorporating advanced radar signal processing techniques.

While the pole-dipole earth resistivity method has demonstrated an early and successful capability for detecting subsurface cavities and tunnels, the ground penetrating radar technique holds a far greater potential for providing more detailed subsurface resolution and a faster ground scanning rate. The development of a ground penetrating radar system capable of reliably scanning and accurately mapping underground cavities and other subsurface anomalies is recommended as a most favorable long range approach to solving problems related to subsurface cavity detection.

A modular radar system design is recommended, allowing the selection of signal frequency and matching antenna to best match the system to the soil and rock medium and penetration depth required in the selected area. This would include special antenna development for borehole measurements. Radar that can penetrate through the walls of a borehole for a distance range of 30 feet (9.1 m) or more would be of great value when suspected tunnels are too far below ground surface to be detected by surface methods.

---

<sup>7</sup> Fountain, Herzig, Owen, loc. cit.

APPENDIX A

BASIC CONCEPTS OF ELECTRICAL EARTH  
RESISTIVITY MEASUREMENTS



## BASIC CONCEPTS OF ELECTRICAL EARTH RESISTIVITY MEASUREMENTS

The basic resistivity measurements and analysis concepts for the various survey methods are essentially the same. If an otherwise predictable electrical current distribution is established within a relatively large volume of homogeneous earth material, perturbations in the current distributions as caused by localized geologic anomalies can be measured as potentials at the ground surface. These anomalous potentials can then be interpreted in terms of possible subsurface structural or earth materials differences.

The basic electrical theory for earth resistivity measurements is discussed and the geometrical factors for several electrode arrays are derived below.

### I. GENERAL THEORY

An electric current distribution can be established within the volume of a conducting earth halfspace by means of a DC or low frequency AC voltage applied to two electrodes in contact with the surface. If the two electrodes are located close together the volume of earth material carrying the major portion of the total current will be relatively small and can be roughly estimated as a hemispherical volume having a diameter about equal to the electrode spacing if the composite earth material can be considered conductively homogeneous. For larger electrode separation distances the depths of the significant current conducting paths increase as does the volume of material carrying the major portion of the total current. Under the idealized condition of a uniformly conducting earth halfspace and in the limit where the separation distance between the two electrodes approaches infinity (i. e., spacing very large compared with the dimensions of the earth material zone containing the current distribution patterns of interest), the current flowing away from a point source electrode diffuses radially into the conducting volume. In this idealized case, the current flow can be considered as diverging away from the source through an infinite number of concentric hemispherical shells representing equipotential surfaces within the medium. At the ground surface, the hemispherical shells form concentric circles about the current electrode at which potential differences between such equipotential shells may be measured.

By Ohm's law, the vector potential gradient between two infinitesimally spaced hemispherical shells is

$$\vec{E} = \rho \vec{J} \quad (A-1)$$

where  $\rho$  = resistivity of the medium; and  
 $\vec{J}$  = vector current density.

For a single current source with its current sink at infinity, all current entering the hemispherical volume from the source must also emerge from that volume and, therefore, the vector current density divergence condition

$$\nabla \cdot \vec{J} = 0 \quad (A-2)$$

must be satisfied. Substituting from Equation (A-1), the Laplace equation for the scalar electric potential is found to be

$$\nabla \cdot \vec{J} = \frac{1}{\rho} \nabla \cdot \vec{E} = 0$$

or

$$\frac{1}{\rho} \nabla^2 \phi = 0 \quad (A-3)$$

where:  $\phi = \int_{\infty}^r \vec{E} \cdot d\vec{l}$  = scalar electric potential.

On the basis of the radial (hemispherical) symmetry already described for a homogeneous conducting earth, Laplace's equation in spherical coordinates is simply

$$\frac{\partial}{\partial r} \left( r^2 \frac{\partial \phi}{\partial r} \right) = 0 \quad (A-4)$$

which, after direct integration, yields the electric field relation

$$r^2 \frac{\partial \phi}{\partial r} = r^2 E = K_1 \quad (A-5)$$

and, after integrating again, the electric potential relation

$$\phi = - \frac{K_1}{r} + K_2 \quad (A-6)$$

where:  $K_1, K_2$  = constants of integration.

At large distances away from the current source electrode ( $r \rightarrow \infty$ ) the potential  $\phi$  must be zero and, therefore,  $K_2 \rightarrow 0$ . Further, if the source current is uniform through a small hemispherical surface about the source electrode then the total current is given by the surface integral

$$I = \int_s \vec{j} \cdot d\vec{s} = \frac{1}{\rho} \int_s \vec{E} \cdot d\vec{s}. \quad (A-7)$$

Substituting from Equation (A-5), the total current becomes

$$I = \frac{K_1}{\rho} \int_s \frac{1}{r^2} ds = \frac{K_1}{\rho} \int_0^{2\pi} d\gamma \int_{-\pi/2}^0 \sin \theta d\theta = -\frac{2\pi K_1}{\rho} \quad (A-8)$$

where

$$ds = r^2 \sin \theta d\gamma d\theta;$$

$\gamma$  = azimuthal angle about current source; and

$\theta$  = polar angle about current source.

Solving for  $K_1$  and substituting into Equation (A-6) gives the scalar electric potential for any hemispherical shell of radius,  $r$ , about a single current source carrying a total current,  $I$ . That is,

$$\phi(r) = \frac{\rho I}{2\pi r}. \quad (A-9)$$

The observable potential difference between two points,  $P_1$  and  $P_2$ , on hemispherical shells concentric about the current source and located at radii,  $r_1$  and  $r_2$  where  $r_2 > r_1$ , is

$$\Delta \phi = \phi(r_1) - \phi(r_2) = \frac{\rho I}{2\pi} \left( \frac{1}{r_1} - \frac{1}{r_2} \right). \quad (A-10)$$

This relationship is important in defining the resistivity of the earth medium when the current sink electrode is located effectively at an infinite distance away from the current source electrode. In this case, the resistivity is

$$\rho = \frac{2\pi}{\left( \frac{1}{r_1} - \frac{1}{r_2} \right)} \quad \frac{\Delta \phi}{I} = K \left( \frac{\Delta \phi}{I} \right) \quad (A-11)$$

where:  $K = \frac{2\pi}{(1/r_1 - 1/r_2)}$  = electrode array geometric factor; and

$$\frac{\Delta\phi}{I} = \text{a measurable ohmic resistance factor.}$$

For the case where the current sink electrode cannot be considered to be located at an infinite distance away from the source electrode, the two equipotential shells used in obtaining Equation (A-10) will no longer be precise hemispheres and the distortion effects on the potentials  $\phi(r_1)$  and  $\phi(r_2)$  caused by the sink electrode must be taken into account. This can be done readily because of the validity of superimposing scalar quantities such as the electric potentials as expressed by Equation (A-9). Thus, if the total sink electrode current is  $-I$  as it must be in a two-electrode arrangement and the distances from the sink electrode to the previously described potential measuring points (located at distances of  $r_1$  and  $r_2$ , respectively, from the source) are  $R_1$  and  $R_2$ , respectively, then the combined potentials at the two measuring points are (for  $R_1, R_2 > r_1, r_2$ ),

$$\begin{aligned} \phi_{p1} &= \phi(r_1) - \phi(R_1) \\ \text{and} \quad \phi_{p2} &= \phi(r_2) - \phi(R_2) \end{aligned} \quad (\text{A-12})$$

The resulting potential difference between the two potential measuring points now becomes,

$$\Delta\phi = \phi_{p1} - \phi_{p2} = \frac{\rho I}{2\pi} \left( \frac{1}{r_1} - \frac{1}{R_1} - \frac{1}{r_2} + \frac{1}{R_2} \right) \quad (\text{A-13})$$

and in this more generalized case the resistivity of the medium is expressed as

$$\rho = \frac{2\pi}{\frac{1}{r_1} - \frac{1}{R_1} - \frac{1}{r_2} + \frac{1}{R_2}} \left( \frac{\Delta\phi}{I} \right) = K' \left( \frac{\Delta\phi}{I} \right) \quad (\text{A-14})$$

where the geometric factor,  $K'$ , for this case differs from  $K$  expressed earlier in Equation (A-11) to take into account the current sink electrode distances.

It is pointed out that the relationships given in Equations (A-13) and (A-14) are general expressions for any electrical resistivity pro-

filing array which utilizes two current electrodes and two potential electrodes as long as the distances  $r_1$  and  $r_2$  represent the magnitudes of the geometric distances from potential electrodes,  $P_1$ ,  $P_2$ , respectively, to the current source electrode  $C_1$  and distances  $R_1$  and  $R_2$  represent the magnitudes of the distances from potential electrodes,  $P_1$ ,  $P_2$ , respectively, to the current sink electrode,  $C_2$ .

## II. THE WENNER ELECTRODE ARRAY

The Wenner electrode array is one of the most widely used arrays for measuring earth resistivity. This array is a four-electrode configuration in which all electrodes are equally spaced along a straight line. The distance between any two adjacent electrodes is defined as the array spacing. The Wenner array electrode configuration is illustrated in Figure A-1. The geometrical factor for the Wenner array is, from Equation (A-14),

$$K_w = \frac{2\pi}{\frac{1}{d} - \frac{1}{2d} - \frac{1}{2d} + \frac{1}{d}} = 2\pi d \quad (\text{A-15})$$

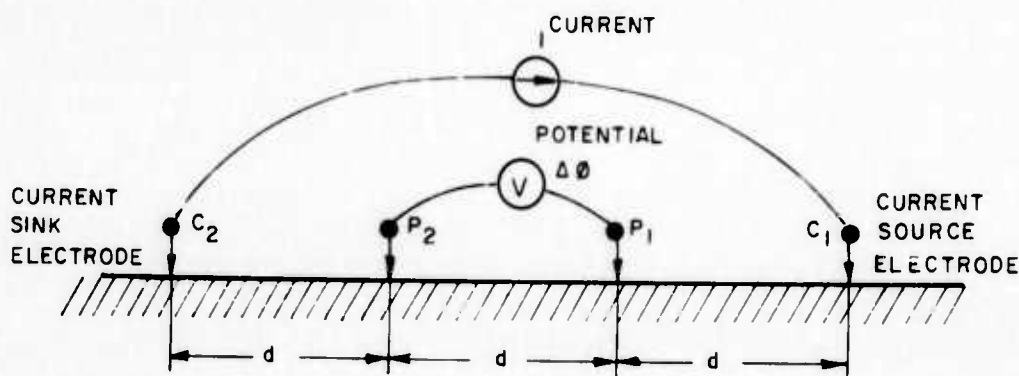


FIGURE A-1. THE WENNER ELECTRODE ARRAY



The geometrical symmetry of this array makes it simple to set up and operate in the field and the simple geometric factor facilitates the interpretation of the observed electrical resistivity measurements.

Referring to Figure A-1, if the current sink electrode were removed to infinity, the hemispherical equipotential shells associated with potential electrodes  $P_1$  and  $P_2$  would have subsurface penetration radii of  $d$  and  $2d$ , respectively. That is, the subsurface earth material affecting the measured resistivity is that contained within the volume bounded by the two hemispherical shells concentrically centered on the source electrode,  $C_1$ . However, the close and symmetrical proximity of the current sink electrode in the standard Wenner array distorts the equipotential surfaces away from their concentric hemispherical shapes and diminishes the depths to which these surfaces penetrate. This apparent reduction in penetration depth for the standard Wenner array compared with the single current electrode case, while phenomenologically correct, is, in part, compensated by the larger potential difference between electrodes  $P_1$  and  $P_2$  resulting from the contribution of the current sink electrode. The apparent maximum penetration response of the Wenner array is oriented directly below the center of the symmetrical array configuration in contrast with the location below the source current electrode when the sink electrode is located at infinity. In practice, the standard Wenner array has its optimum response to large resistivity anomalies when they are located at a subsurface depth approximately equal to the array spacing dimension. Because of the relatively large volume of earth material embraced by the equipotential surfaces terminating at electrodes  $P_1$  and  $P_2$  and surrounding the two current electrodes, the Wenner array tends to provide a larger volume resistivity average and a lower resolving power for small anomalies than certain other electrode configurations. For this reason, the Wenner array has been most applicable in geophysical surveys requiring depth sounding and resistivity measurements related to large subsurface earth stratification conditions. While it has also been used as a fixed-depth horizontal profiling technique (i. e., array spacing held constant and the entire array moved horizontally over the ground surface) for detecting vertical earth structural formations such as dikes and cavities, there are other electrode array configurations that exhibit greater depth sensitivity and resolution for such anomalies.

### III. THE POLE-DIPOLE ARRAY

The pole-dipole earth resistivity electrode configuration consists of a current source electrode (pole) and a potential electrode pair (dipole) oriented in a straight line array. The current sink electrode is

located sufficiently far from the source electrode that its effects on the potential values observed by the dipole electrode pair are negligible. The details of this electrode array configuration and a description of its operation is presented in Section IV and illustrated in Figure 9 in the main body of this report.

The geometrical factor for the pole-dipole array is derived from the general expression in Equation (A-14) for the conditions  $R_1 \rightarrow \infty$  and  $R_2 \rightarrow \infty$  corresponding to the location of the current sink electrode at an infinite distance from the potential electrodes. Thus, the geometric factor for the pole-dipole array is,

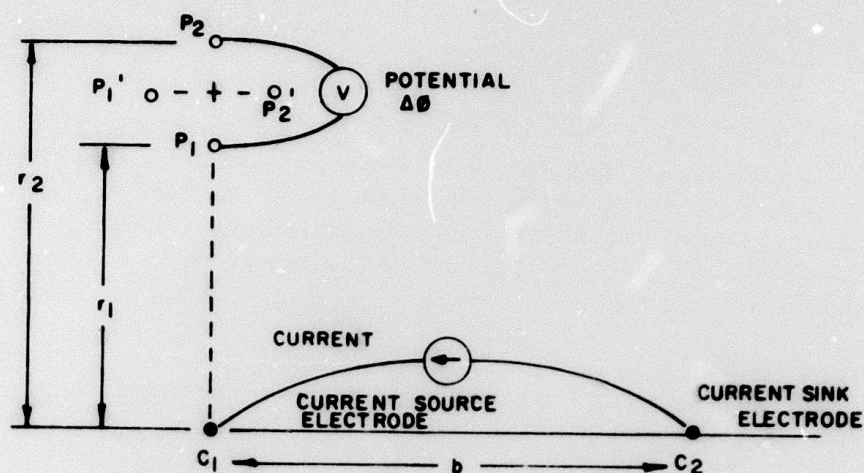
$$K_{P-D} = \frac{2\pi}{\frac{1}{r_1} - \frac{1}{r_2}} = \frac{2\pi r_1 r_2}{r_2 - r_1} \quad (A-16)$$

#### IV. THE L-SHAPED ARRAY

The L-shaped electrode array is comprised of a wide-spaced current electrode pair located along the lower arm of the "L" pattern and a closely spaced fixed-dimensional potential electrode pair oriented and scanned along the upper perpendicular arm of the "L" at logarithmically-spaced intervals. The source current electrode is located closest to the potential electrode pair at the corner of the "L" and the sink electrode is located at the outer extreme point on the lower arm of the "L". The L-shaped array is illustrated in plan view in Figure A-2.

In general the current sink electrode of this array is not considered to be located at an infinite distance away from the current source or potential measurement electrodes. However, if such a condition is permitted then the electrode configuration of the L-shaped array reduces essentially to that already described for the pole-dipole array (and for other similar array configurations such as the half-Schlumberger array used by previous investigators). The exact geometric factor for the L-shaped array is, from Equation (A-14)

$$K_L = \frac{r_2 - r_1}{r_1 r_2} - \left[ \frac{\frac{2\pi}{\sqrt{r_2^2 + b^2}} - \frac{2\pi}{\sqrt{r_1^2 + b^2}}}{\frac{2\pi}{\sqrt{r_1^2 + b^2}} - \frac{2\pi}{\sqrt{r_2^2 + b^2}}} \right] \quad (A-17)$$



THE L-SHAPED ELECTRODE ARRAY

FIGURE A-2. THE L-SHAPED ELECTRODE ARRAY

where:  $b$  = distance between current electrodes.

As may be noted from Equation (A-17) above when  $b \rightarrow \infty$  the geometric factor for the L-shaped array approaches that given earlier in Equation (A-16) for the pole-dipole array.

It has been shown by Zohdy<sup>(8)</sup> that the L-shaped array configuration has advantages and flexibility in the positioning of the current sink electrode, especially on long or deep sounding resistivity surveys, and that its resistivity sensitivity to stratified earth structures is intermediate between that of an ideal equatorial dipole array and an ideal polar dipole array\*. That is, the perpendicular orientation of the cur-

<sup>8</sup> A. A. R. Zohdy, "Electrical Resistivity Sounding with a L-Shaped Array," U. S. Geological Survey Bulletin 1313-C, 1970.

Note: An ideal equatorial dipole array is one in which the distance  $b \rightarrow 0$  and the distance  $(r_2 - r_1) \rightarrow 0$  in Figure A-2 and then the potential electrodes are repositioned to be parallel to  $b$ , i. e., at  $P_1$  and  $P_2$ . An ideal polar dipole array is one in which the position of the potential electrodes,  $P_1$  and  $P_2$ , in Figure A-2 remains unchanged but the sink electrode,  $C_2$ , is placed on the vertical traverse arm of the "L" and the distance between  $C_1$  and  $C_2$  is allowed to approach zero. Comparisons of these ideal array configurations have been analyzed by Keller<sup>9</sup>.

<sup>9</sup> G. V. Keller, "Dipole Method for Deep Resistivity Studies," *Geophysics*, 31, 1088-1104, 1966.

rent and potential electrode pairs in the L-shaped array has a deeper probing depth sensitivity than the polar dipole array (but not as great as that of an equatorial dipole array), and it has a stronger apparent resistivity response than the equatorial dipole array (but not as strong as that of a polar dipole array.)

A variation of the L-shaped array as described above is one in which the potential electrode pair is oriented at points  $P_1'$  and  $P_2'$  as shown in Figure A-2 and scanned in this fixed orientation along the upper arm of the "L". In this case, the electrode pair is not responsive to the current distribution produced by the source electrode,  $C_1$ , under assumed homogeneous earth conditions because of the location of both  $P_1'$  and  $P_2'$  on a single equipotential hemispherical shell which would surround  $C_1$  if  $C_2$  were at infinity. However, this electrode pair is otherwise responsive to the current distribution produced by the current sink electrode and can be used as a measure of the perturbing influence of the current sink electrode on the current distribution produced by the source electrode as observed in the standard L-shaped array. This procedure is useful in transforming the L-shaped array apparent resistivity readings to those obtainable with the sink electrode located at infinity. By this method the infinite distance sink electrode can be avoided and the transformed resistivity will correspond to the resistivity data available in Schlumberger albums<sup>10</sup> of theoretical resistivity curves for various subsurface cases.

By way of further discussion, the more generalized use of the L-shaped array using special orientations of the potential electrode pair as described above, makes it possible to measure the "x" and "y" components of apparent resistivity. Analysis of these components and the resultant "total" apparent resistivity can yield information on the anisotropy of the subsurface earth materials, and, more importantly, can aid in interpreting the possible shape of detected localized anomalies including elongated cavity structures.

As with the other resistivity survey methods, the L-shaped array can be operated either as a vertical resistivity sounding array or as a horizontal profiling array. By combining both of these functions to gather a large amount of overlapping data, the L-shaped array can possibly provide a resistivity survey method having special advantages in certain survey applications. The major advantages to

---

<sup>10</sup>"Master Curves for Electrical Soundings," Compagnie Generale de Geophysique, The Hague, European Assoc. Explor. Geophysicists, 1963.



be gained by this method are in eliminating the need for the infinite distance current sink electrode and in providing interpretive information on the anisotropic resistivity signatures of elongated solution cavity structures or man-made underground mining excavations of interest.

## V. A SWITCHED-ELECTRODE EQUATORIAL DIPOLE ARRAY

In a previous investigation pertaining to the detection of shallow man-made tunnels, Southwest Research Institute tested an unconventional electrical resistivity survey method intended to emphasize the response to small subsurface tunnels and to simplify the required resistivity interpretation requirements.<sup>11</sup> The work on this method was a limited effort aimed at: (1) establishing the feasibility of the method for detecting tunnels; (2) evaluating its performance in comparison with a standard resistivity method (a Wenner array); and (3) evaluating the method using rolling-contact metallic electrodes.

The switched-electrode equatorial dipole array was first conceived as a vehicle wheelbase-size electrode array whereby the necessary current source, potential measuring instrument, switching circuits, and data recording and output display equipment would be carried as part of a single vehicle-mounted survey system. The electrodes of the array would be mounted as part of the vehicle wheels as a means for continuous mobile resistivity surveying over suitable off-road terrain. With this method, the penetration depth of the current distribution patterns would only be comparable with the wheelbase and/or track width dimensions of the electrode array; however, such depths were considered adequate for the intended tunnel detection application. The exceptional results obtained with the simplified test version of this concept in detecting typical man-made tunnels in the San Antonio vicinity were encouraging enough to suggest the use of this method on a larger scale for subsurface cavity detection related to other survey applications.

Figure A-3 illustrates the general electrode configuration required in the switched-electrode array. On one half of the switching cycle (solid lines), electrodes E<sub>1</sub> and E<sub>4</sub> comprise a current dipole of spacing,  $a$ , and electrodes E<sub>2</sub> and E<sub>3</sub> comprise a potential measuring dipole of spacing,  $a$ , separated at a distance,  $b$ , from the current dipole. On the alternate half of the switching cycle (dotted lines), electrodes E<sub>1</sub> and E<sub>2</sub> comprise a current dipole of spacing,  $b$ , and electrodes E<sub>3</sub> and E<sub>4</sub> comprise a potential measuring dipole of spacing,  $b$ , separated at a distance,  $a$ , from the current dipole. The spatial orientation of the equatorial dipole array pattern established on the alternate switching half cycle is rotated 90 degrees from that established on the first half cycle.

---

<sup>11</sup> Fountain, loc. cit.



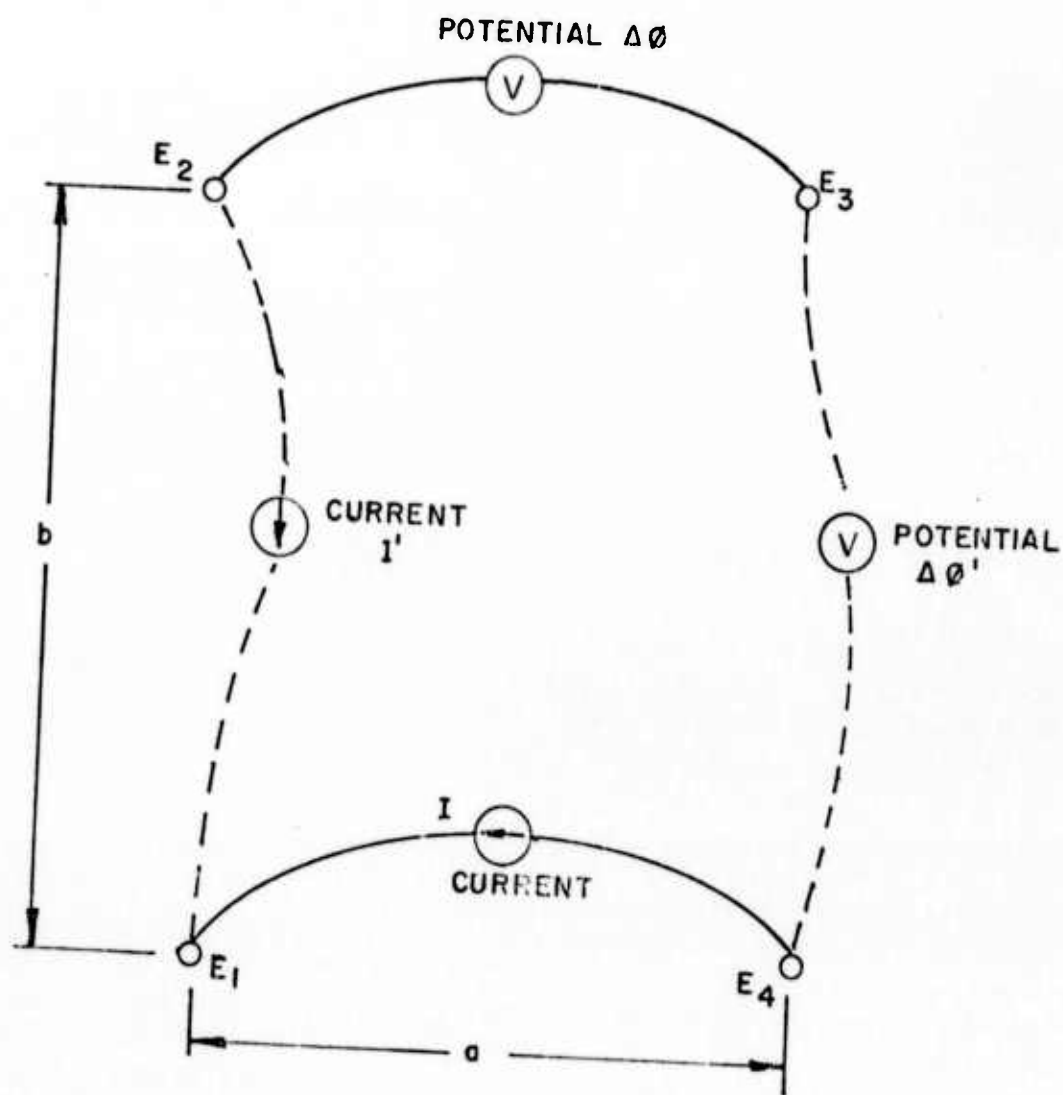


FIGURE A-3. THE SWITCHED-ELECTRODE EQUATORIAL DIPOLE ARRAY

The geometric factors for the two half cycles of switched operation are:

For  $E_1$  = current source electrode  
 $E_4$  = current sink electrode  
 $E_2, E_3$  = potential electrodes,

$$K_{ED} = \frac{2\pi}{\frac{1}{b} - \frac{1}{\sqrt{a^2+b^2}} - \frac{1}{\sqrt{a^2+b^2}} + \frac{1}{b}} = \frac{\pi b \sqrt{a^2+b^2}}{\sqrt{a^2+b^2} - b} \quad (A-18)$$

and for

$E_1$  = current source electrode

$E_2$  = current sink electrode

$E_4$ ,

$E_3$  = potential electrodes ,

$$K'_{ED} = \frac{2\pi}{\frac{1}{a} - \frac{1}{\sqrt{a^2+b^2}} - \frac{1}{\sqrt{a^2+b^2}} + \frac{1}{a}} = \frac{\pi a \sqrt{a^2+b^2}}{\sqrt{a^2+b^2} - a} \quad (A-19)$$

For the case of a square electrode pattern, the two geometric factors are equal. That is, for  $a = b$ ,

$$K_{ED} = K'_{ED} = \frac{\pi \sqrt{2} a}{\sqrt{2} - 1} \quad (A-20)$$

The switching process was incorporated into the original resistivity tunnel detection concept for two reasons. The first was to eliminate the need for calculating and interpreting the survey data in terms of absolute observed apparent resistivity when only the anomalous variations were of interest. This could be achieved through the switching process by subtracting the resistivity values derived on each half cycle of operation to obtain a detected resistivity difference. In this manner, the possible wide range of magnitudes of resistivity encountered in different soils would not be involved in the survey operator's interpretation process. The second reason for switched-electrode operation was to provide a change of array orientation as the survey progressed in order to obtain resistivity responses from more than one observational aspect. As found in the field tests, the wheelbase electrode array exhibited significantly different apparent resistivities in the presence of a tunnel target for each half of the switching cycle because of the elongated nature of the tunnel related to the array pattern. Thus, by switching the electrode orientation progressively along the traverse, the chances of missing an arbitrarily oriented tunnel target because of an

inappropriate array aspect would be reduced. In addition to these two advantages of the switching process, it was also found in the course of the field tests that, for 90-degree electrode array switching as illustrated in Figure A-3, the apparent resistivity anomaly functions obtained on each half cycle were complementary in form. Thus, when the difference between the two resistivities was obtained, it resulted in a stronger net anomaly than that exhibited by either half cycle alone.

The average difference resistivity obtained by the method of electrode switching which includes subtracting the apparent resistivities observed on each half cycle and filtering the cyclic switching frequency components is

$$\Delta \rho_{a,b} = \rho - \rho' = K_{ED} \frac{\Delta \theta}{I} - K'_{ED} \frac{\Delta \theta'}{I} \quad (A-21)$$

for the electrode switching arrangement shown in Figure A-3 and for the case of constant current,  $I$ , flowing in each switched current dipole pair. Substituting the geometric factors from Equations (A-19) and (A-19) gives

$$\Delta \rho_{a,b} = \frac{\pi \sqrt{a^2 + b^2}}{I} \left[ \frac{b \Delta \theta}{\sqrt{a^2 + b^2} - b} - \frac{a \Delta \theta'}{\sqrt{a^2 + b^2} - a} \right] \quad (A-22)$$

Because of the difference in array factors the net resistivity is not zero in Equation (A-23) for the case of a homogeneous earth medium; however, this difference is, on the average, a constant value which changes relatively slowly along the traverse and could be nulled out by subtracting a longer term average of the difference resistivity,  $\Delta \rho_{a,b}$  if desired.

Another advantage offered by the rectangular electrode array lies in the fact that each half of cycle of switched operation offers a slightly different resistivity penetration depth. Thus, the probing depth of the composite switched-electrode array is optimized for a wider range of target depths than either one of the switched arrays alone.

For the case of a square electrode array pattern, the average difference resistivity obtained by the signal processing technique described above is, for  $a = b$ ,

$$\Delta \rho_{a,a} = \frac{\pi \sqrt{2} a}{(\sqrt{2} - 1) I} (\Delta \theta - \Delta \theta') \quad (A-23)$$

Thus, for a square switched-electrode array pattern, the observed difference resistivity is proportional to the difference between the potentials measured on each half of the switching cycle. This difference clearly approaches zero for the condition of a homogeneous earth material containing no anomalies. However, when an arbitrarily oriented anomaly such as a cavity is approached along a survey traverse, the difference between the apparent resistivity responses of the two arrays will reveal the presence of such a target. Moreover, this target indication will be further enhanced by any anisotropic resistivity effects such as those exhibited by an elongated cavity structure.